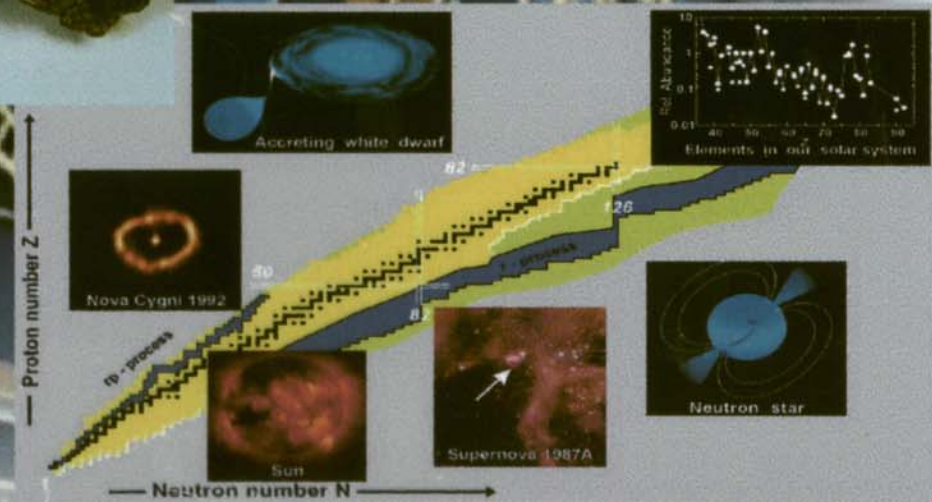
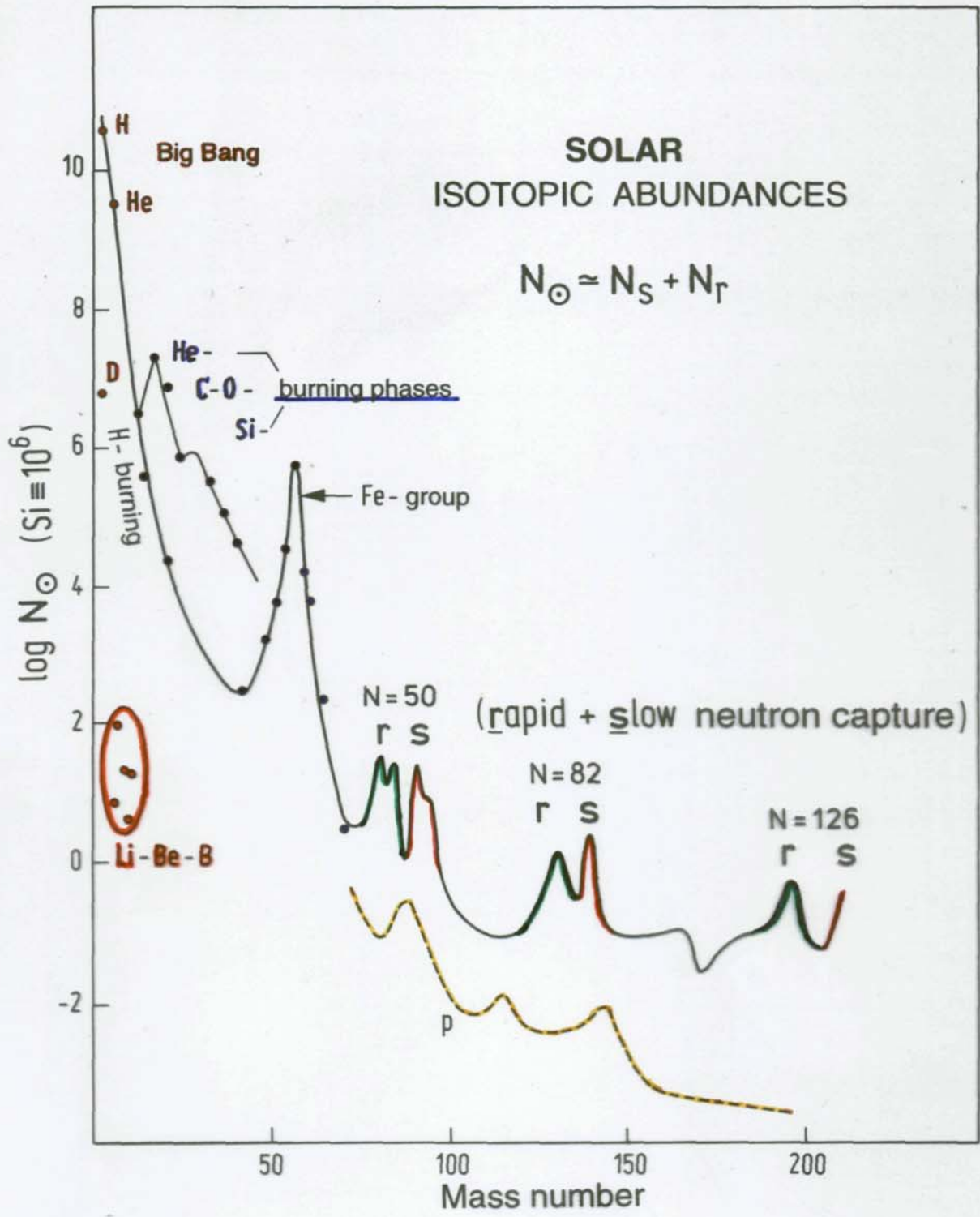


R-Process Signatures: Observations versus Predictions



K.-L. Kratz
Institut für Kernchemie
Universität Mainz, Germany





r-process

Supernova II

moderate n -densities ($n_n \approx 10^{23}$)
explosive (He, C, Si) shell burning
high-entropy bubble, core scenario

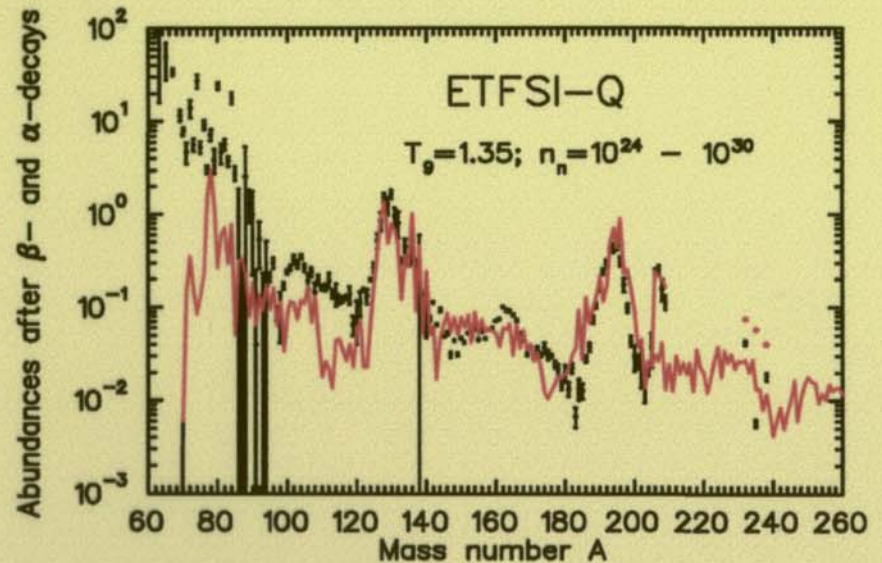
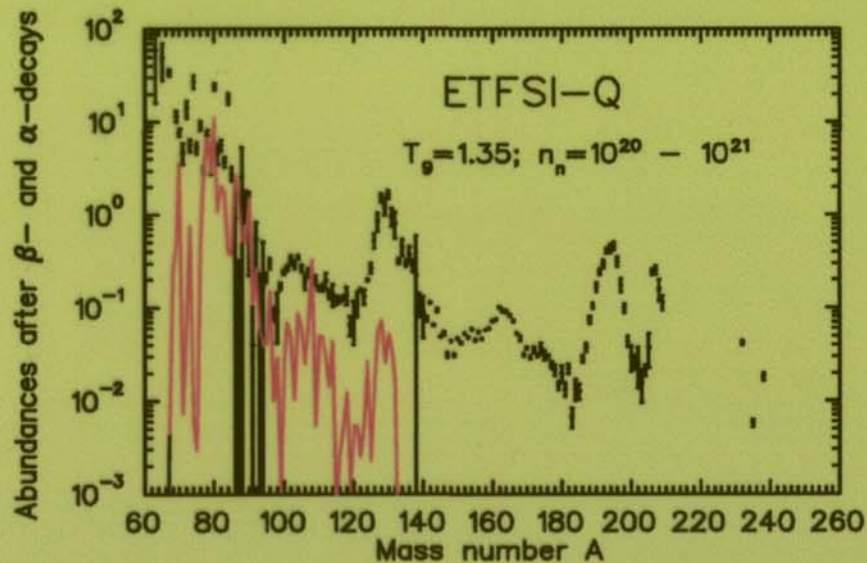
Neutron Star Mergers

high n -densities ($n_n \approx 10^{30}$)
very n -rich ejecta
fission "recycling"

nuclear data needs

direct: $Q_\beta, S_n, T_{1/2}, P_n, \sigma_{n\gamma}$ on "waiting-point nuclei" at N_{mag}

indirect: development of nuclear structure with isospin



Observations r-Nucleosynthesis

Solar-system **isotopic** r-abundances ($N_{r,\odot} \simeq N_{\odot} - N_{s,\odot}$)

Arlandini et al., 1999

Elemental r-abundances in UMP Halo stars

Cowan et al., 1999

Cayrel et al., 2001

Isotopic r-abundances in MP Halo stars

Snedden et al., 2002

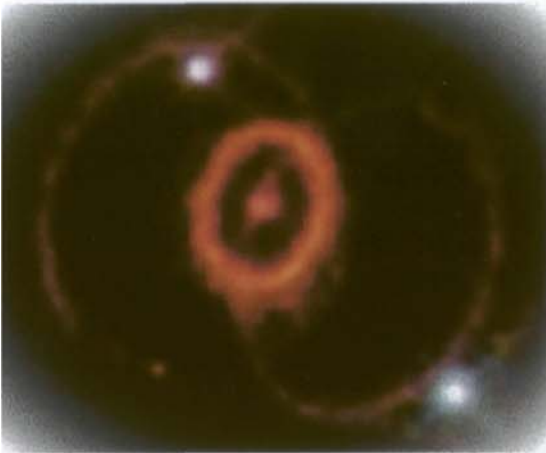
Lambert et al., 2002

Isotopic abundance anomalies in Meteorites

Wasserburg et al., 1977

1996

Ott et al., 1996



Calculations r-Process „Observables“

Time-dependent, classical „**waiting-point**“ model

Kratz et al., 1993

Experimental and microscopic-model nuclear-data input

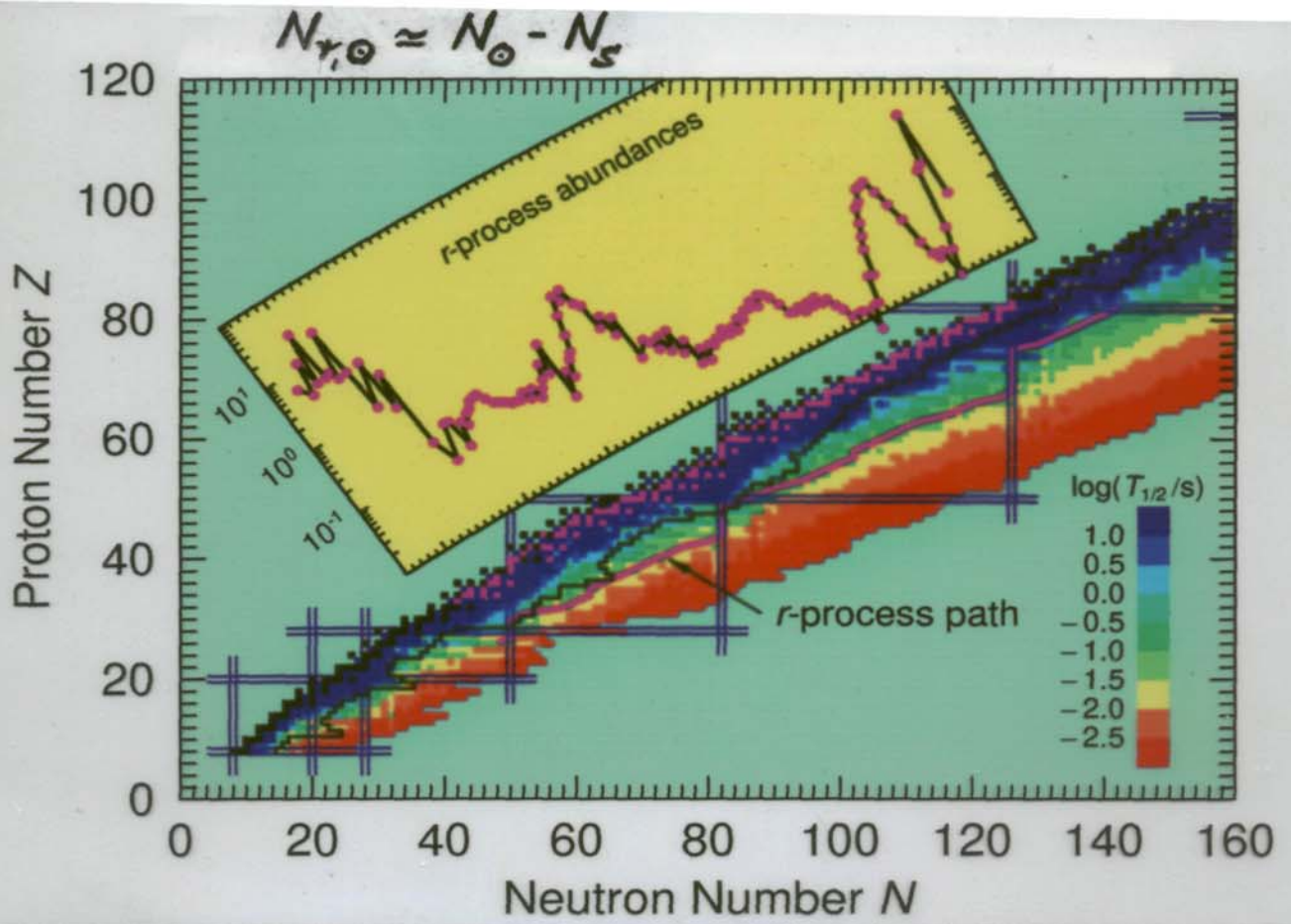
Pfeiffer et al., 2001

Möller et al., 2002

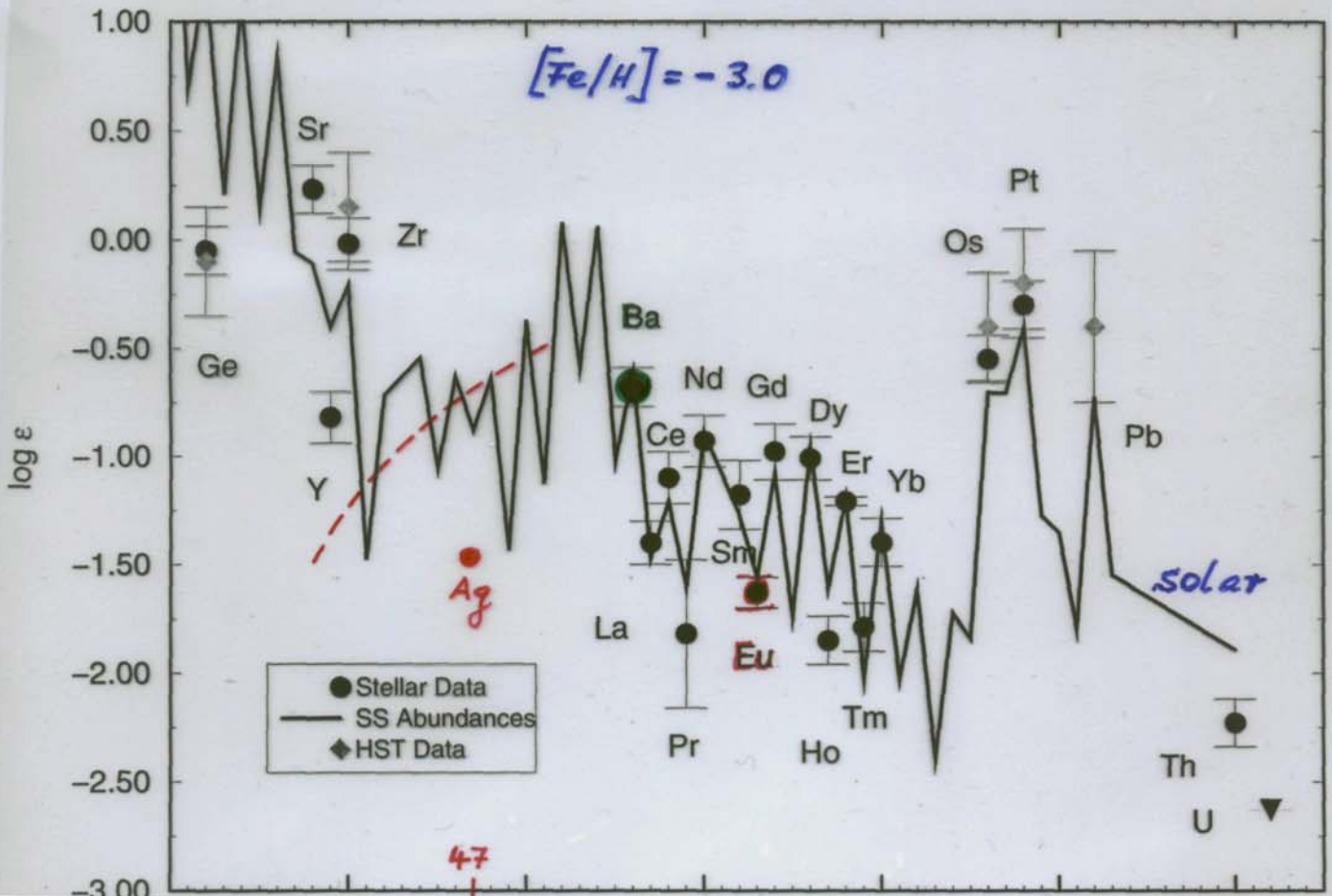
High-entropy bubble, full dynam. network

Freiburgh. et al. 1999

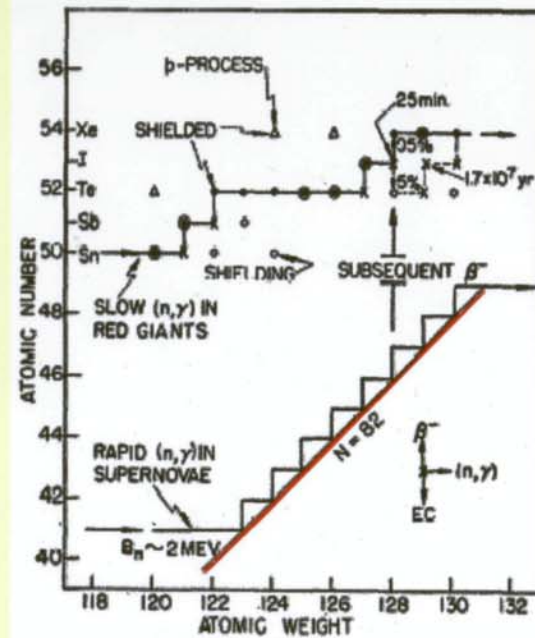
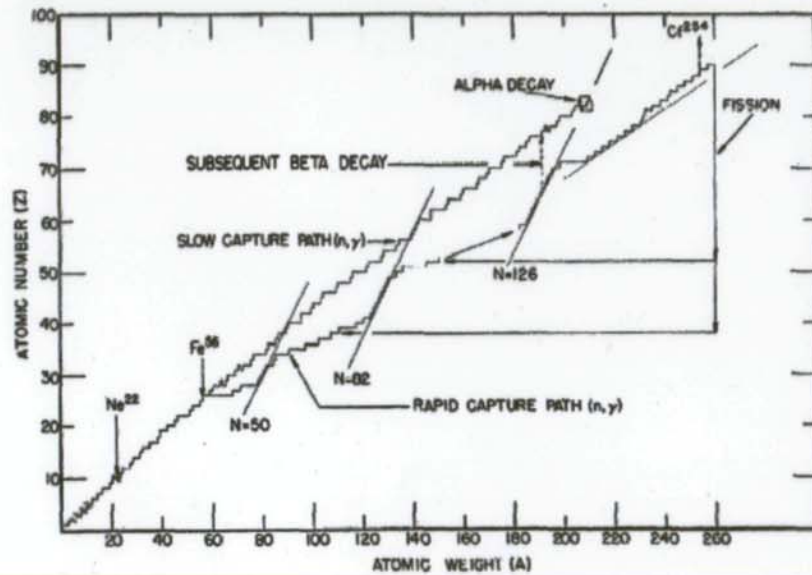
Farouqi 2003



Low-Metallicity Giant HD 115444



R-process at magic numbers



B²FH predicted correctly even the detailed behaviour at N=50, 82 and 126.

The „climb up the staircases“, the major waiting-point nuclei involved, as well as the „break-through pairs“, and their „association with the rising sides of major peaks in the abundance curve for the r-process“ are still today important properties to be studied experimentally and theoretically.

J. Phys. G 24 (1988)

With $T_{1/2}(\text{exp})$ and $N_{r,0}$

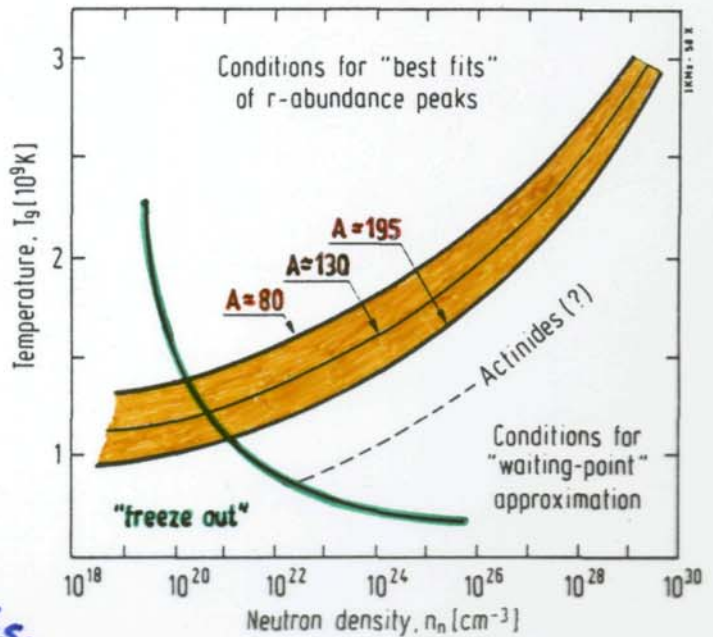
test of

"waiting-point concept":

correlate $T_{1/2} \Leftrightarrow N_{r,0}$

deduce $T_g - n_n$ band

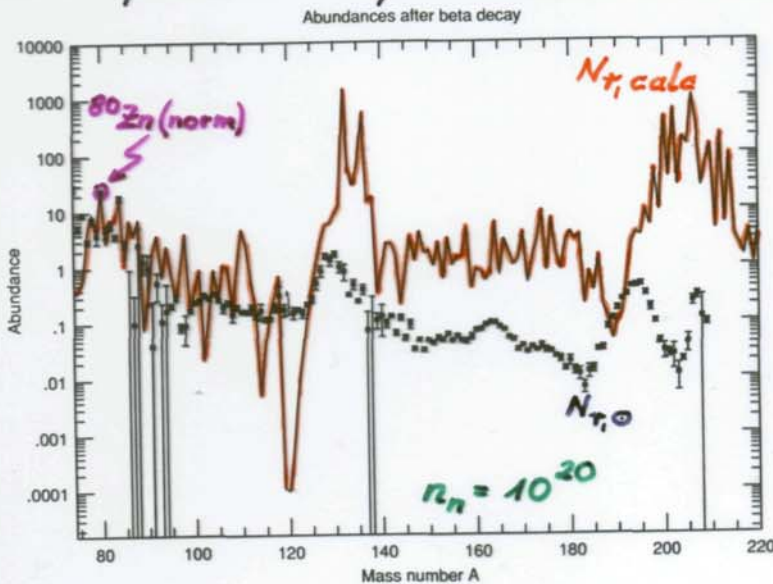
conditions to fit the $A \approx 80$ and 130 $N_{r,0}$ -peaks.



Ap. J. 403 (1993)

Static and time-dependent r-process calculations for "freeze-out" conditions.

Use of internally consistent nuclear-physics input (FRDM + QRPA).

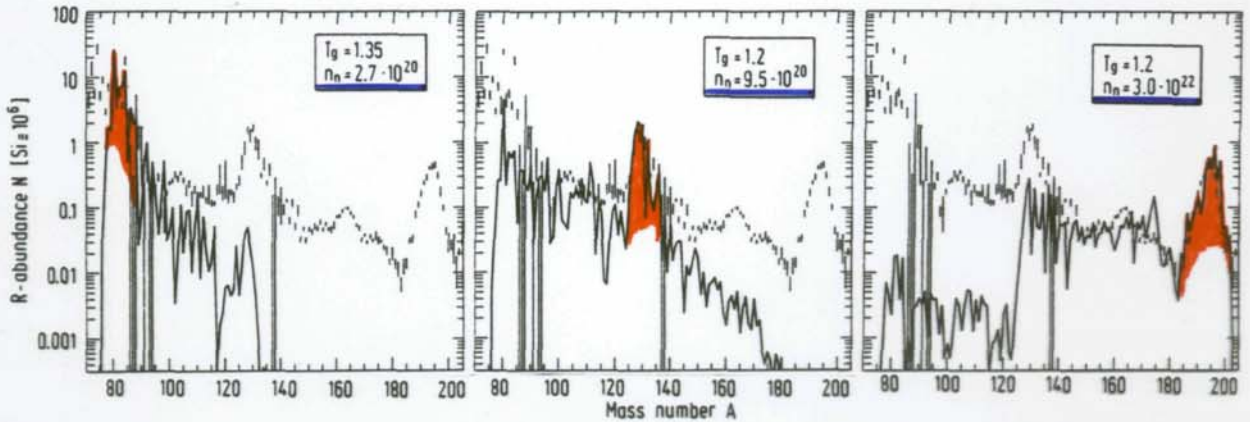


Steady-flow NOT global

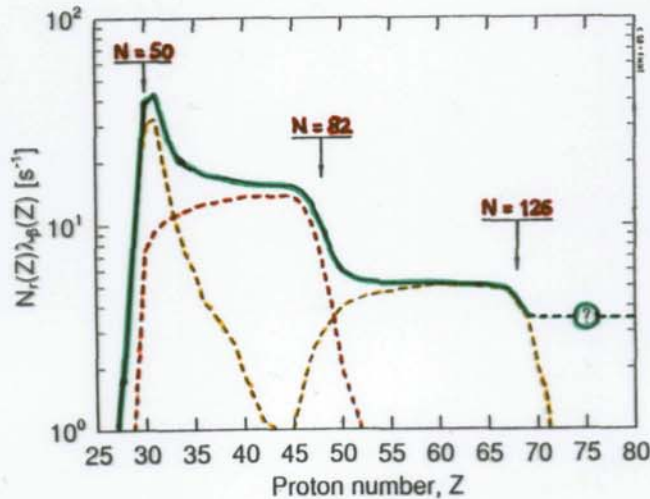
- wrong trend, increasing N_r with A
- $A \approx 130$ and 135 peaks shifted, too large;
- indicates too low n_n

Consequences:

- r -process must have several components with different n -densities and different r -process paths.



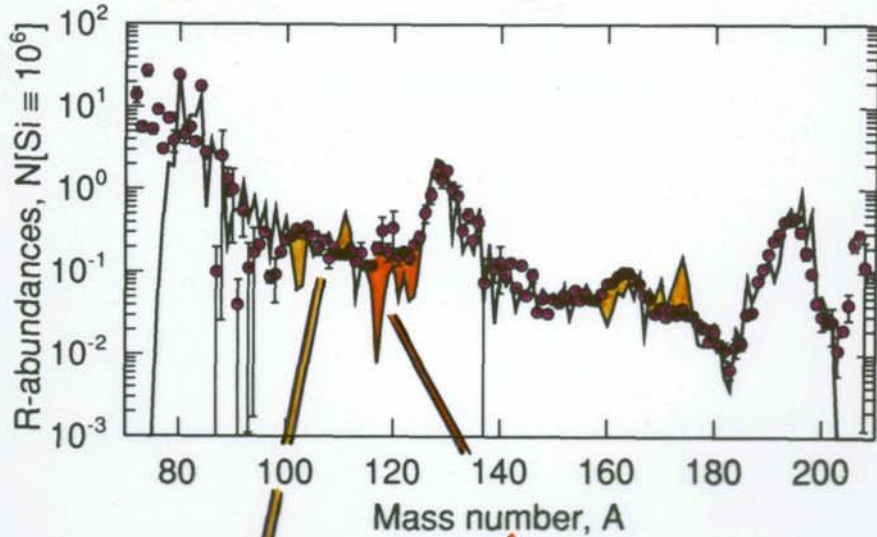
- steady-flow is only local, breaks down at each N_r -peak \rightarrow at N_{magic}



analogous to s -process with $N_s G = \text{const.}$
 empirical r -process picture with superposition of (minimum) 3 components

Superposition of 3 components

→ good overall agreement with $N_r(0)$



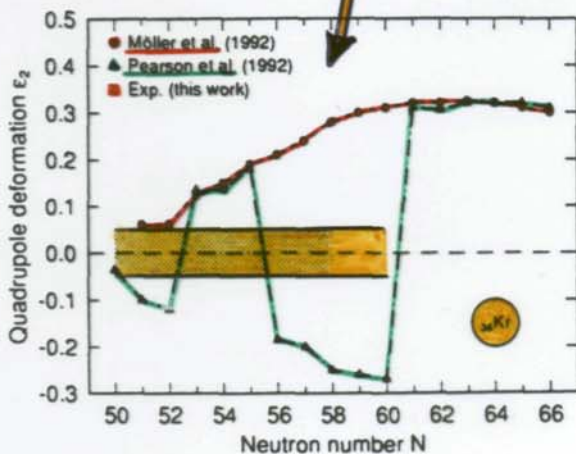
but...

Local deficiencies

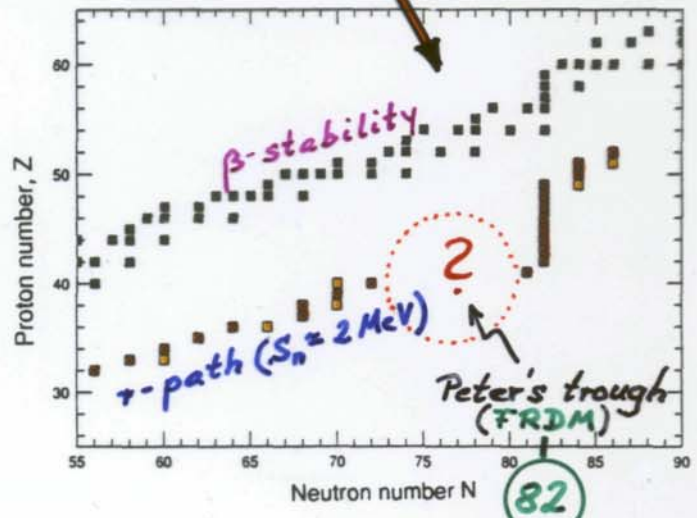
interpreted as nuclear-structure signatures of r -isotopes not accessible in terrestrial laboratories

⇒ model deficiencies!

(i) phase transitions
pn-residual interact.



(ii) shell corrections
 $N=50, 82, 126$



Conclusion

“waiting-point” concept

with $(n,\gamma)\Leftrightarrow(\gamma,n)$ and β -flow equilibrium

and $T_g=\text{const.}$, $n_n=\text{const.}$, instant. freeze-out

is valid.

simple, good “working horse” for parameter studies!

However,

- ❖ steady flow **not** global
⇒ need more than 1 r-component
- ❖ from Fe-seed, $\tau_t \geq 3.5 \text{ s} \Rightarrow$ **too long?**
- ❖ $n_n \approx 10^{20} - 10^{28} \text{ cm}^{-3} \Rightarrow$ **too high?**
- ❖ **nuclear structure far off β -stability?**

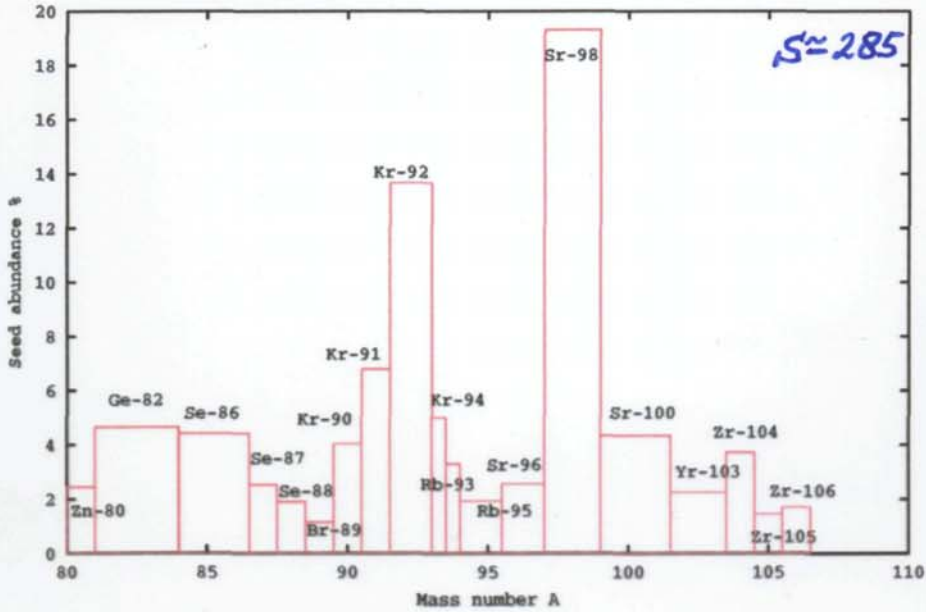
Requests:

1. better r-process models
2. better nuclear structure models
3. **experiments**

After α -process ...

r-process seed

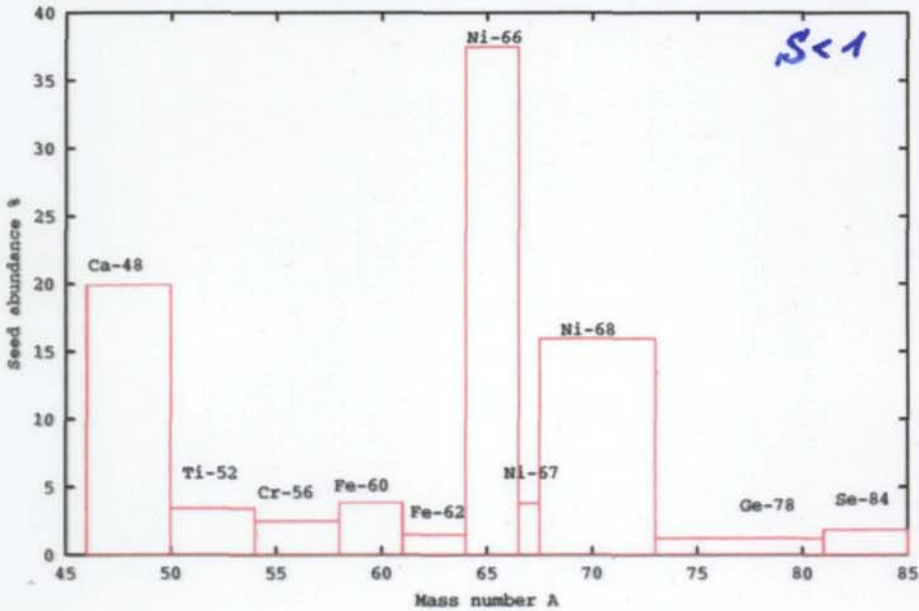
Typical seed nuclei distribution after an alpha-rich freezeout



Subsequent
r-process?

yes!

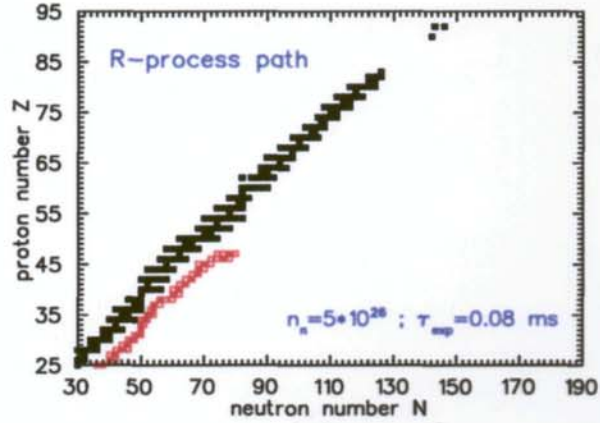
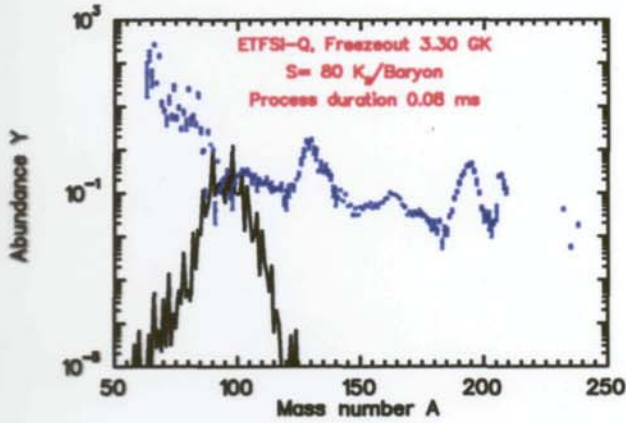
Typical seed nuclei distribution at very low entropies ($S \ll 1$), $(Y_n/Y_{seed}) = 1E-6$



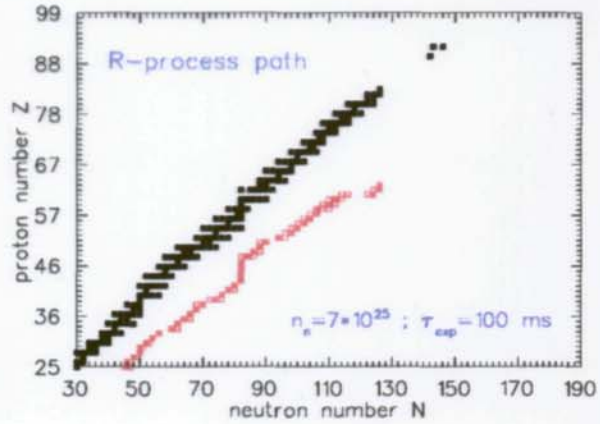
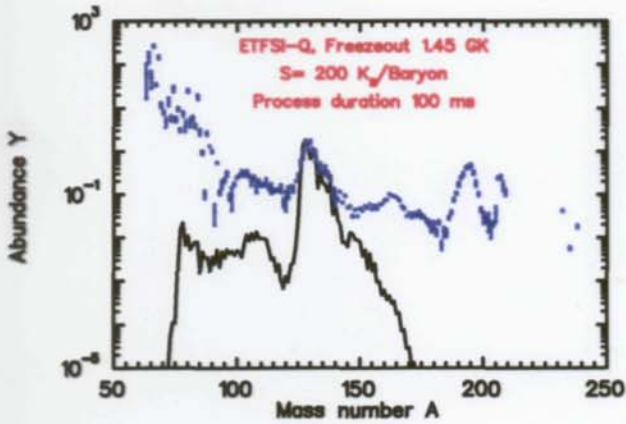
no!

Subsequent r-process for $V_{exp} = 4500 \text{ km/s}$ and $Y_e = 0.43$

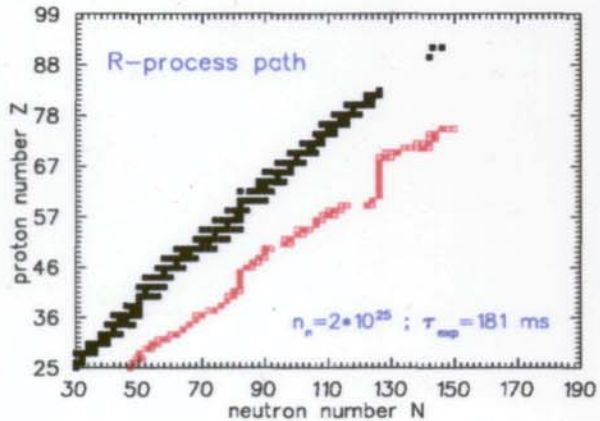
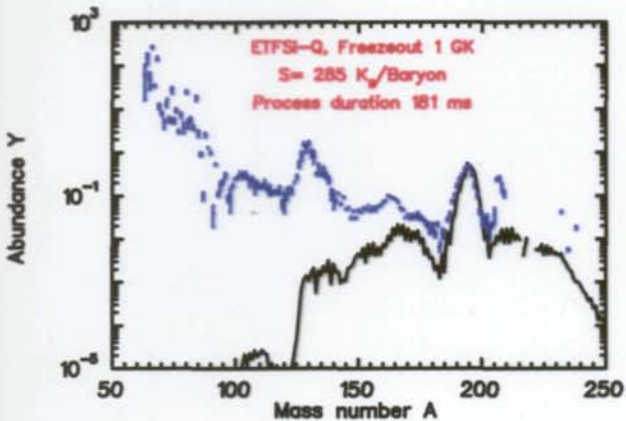
A=90-Peak, $\frac{Y_n}{Y_{seed}} = 1$



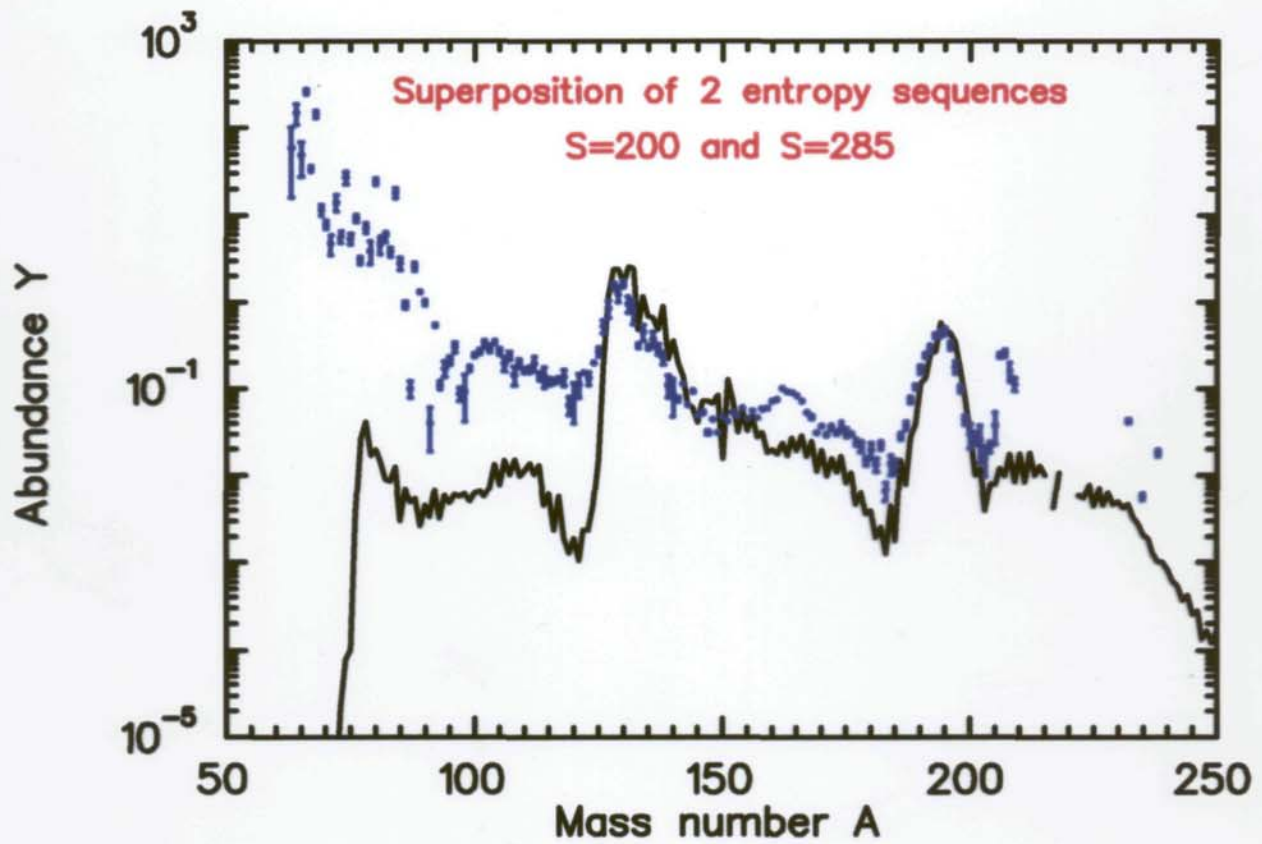
A=130-Peak, $\frac{Y_n}{Y_{seed}} = 34$



A=190-Peak, $\frac{Y_n}{Y_{seed}} = 100$



Superposition of different entropy sequences for $Y_e = 0.43$



Fit function: $g(S_i) = a_1 e^{a_2 S_i} \quad i = 1, \dots, 20$

Fit parameter: $a_1 = 100, \quad a_2 = 1, 2 \times 10^{-2}$

Conclusions

High-entropy neutrino-wind scenario with an initial α -process and a subsequent r-process more realistic, but more time-consuming to calculate

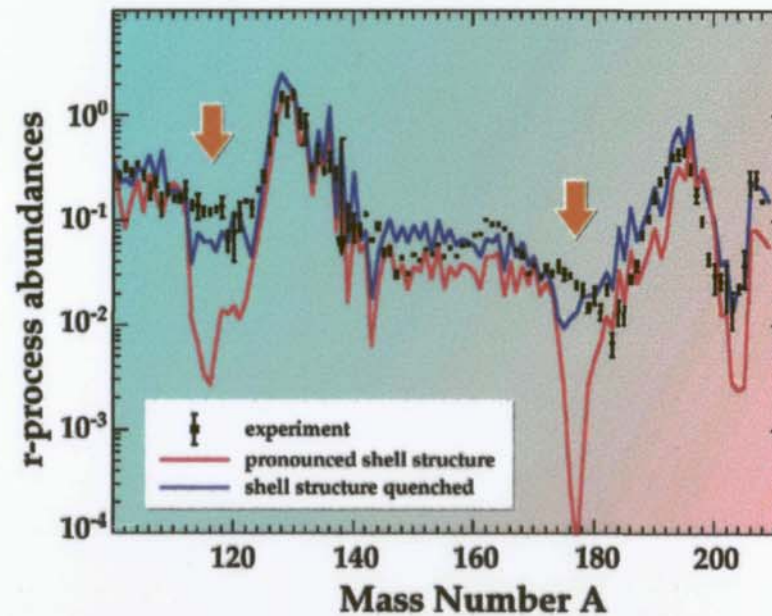
Analytical relation of parameters

$$\frac{Y_n}{Y_{seed}} = k_{SN} V_{\text{exp}} \left(\frac{S}{Y_e} \right)^3$$

- again, need more than 1 r-component
- again, need high $n_n // S$
- no longer Fe-seed; n-rich $A \approx 90$ avoids $N=50$ “bottle-neck” for r-matter flow
- r-process duration 200 ms

Shell Quenching?

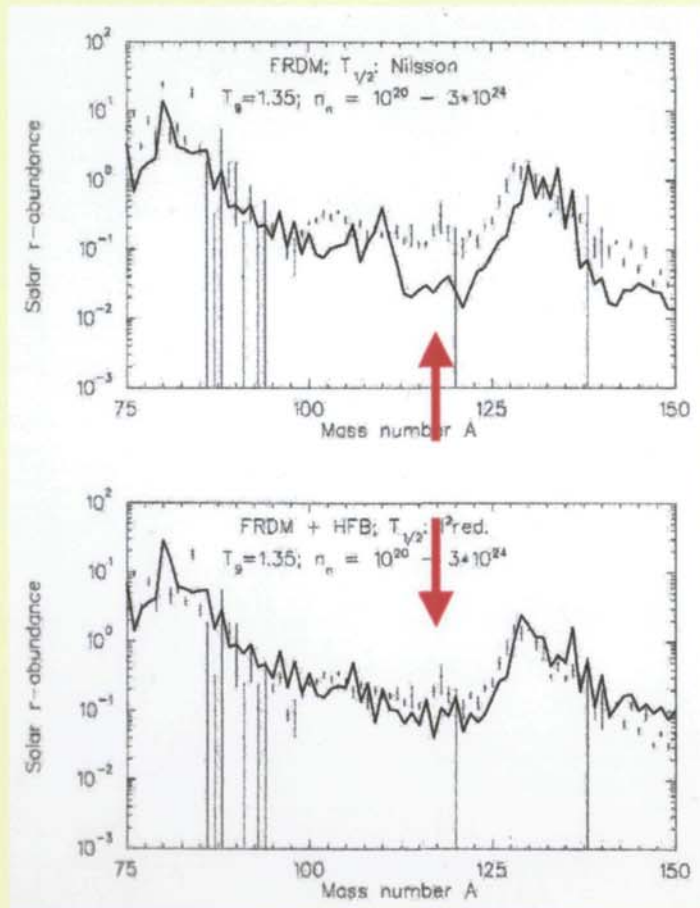
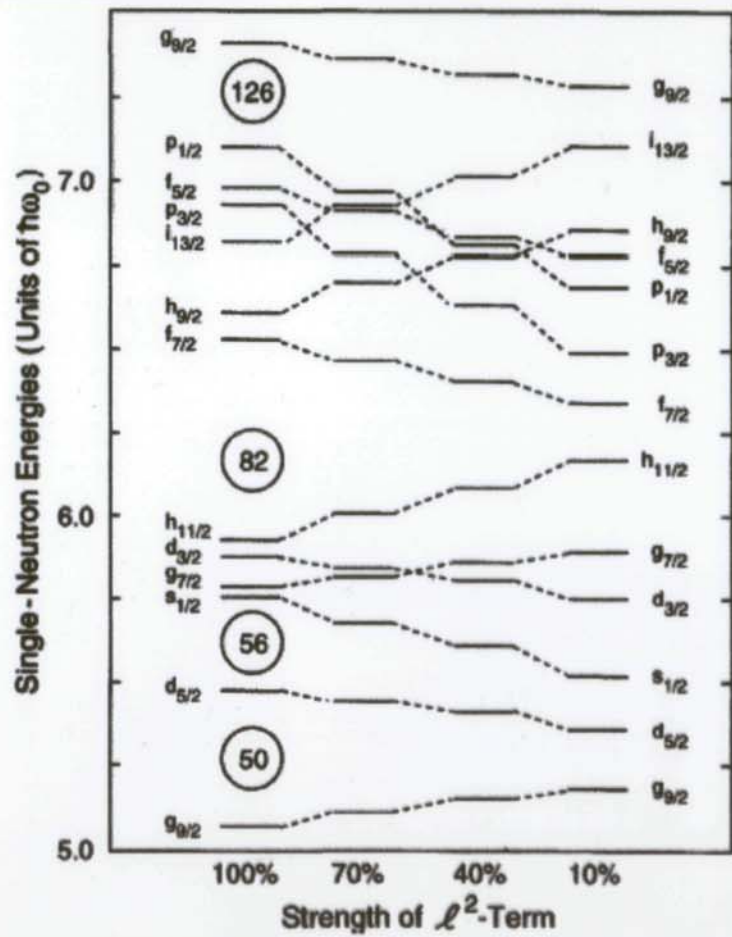
Deficiencies prior to the main peaks were attributed by our group to nuclear structure effects: too strong shell strength for neutron-rich magic nuclei far from stability



Question:

Can one learn neutron-dripline physics from astrophysical observables?

- The weakening (quenching) of the shell gaps can be simulated by reducing the l^2 -term in the Nilsson potential
- The trough in the abundances prior to $N=82$ vanishes



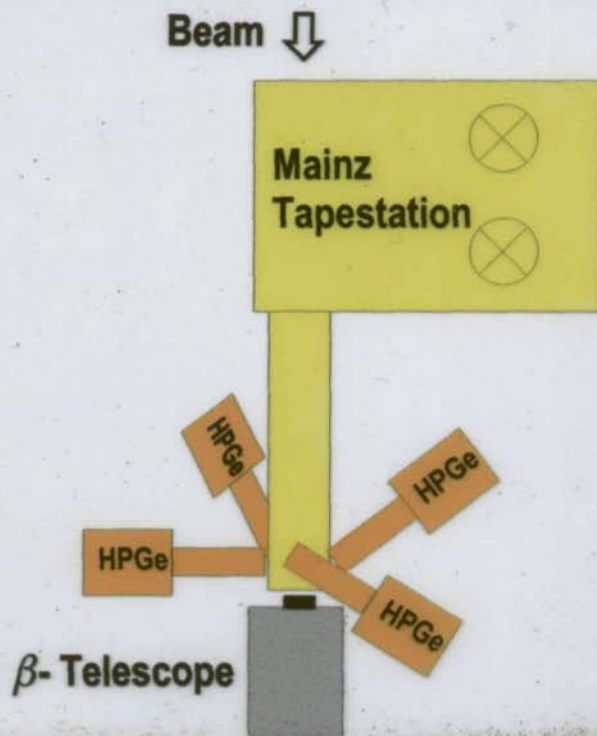
Motivation for r-Process-Experiments

- 1 Direct information**
(Q_β , S_n , $T_{1/2}$, P_n)
of "waiting-point" isotopes in the r-path.
- 2 Indirect information**
nuclear-structure development
(Q_β , E_{level} , ϵ_2 , shell-closures, etc.)
towards the r-path.

Regions of major interest

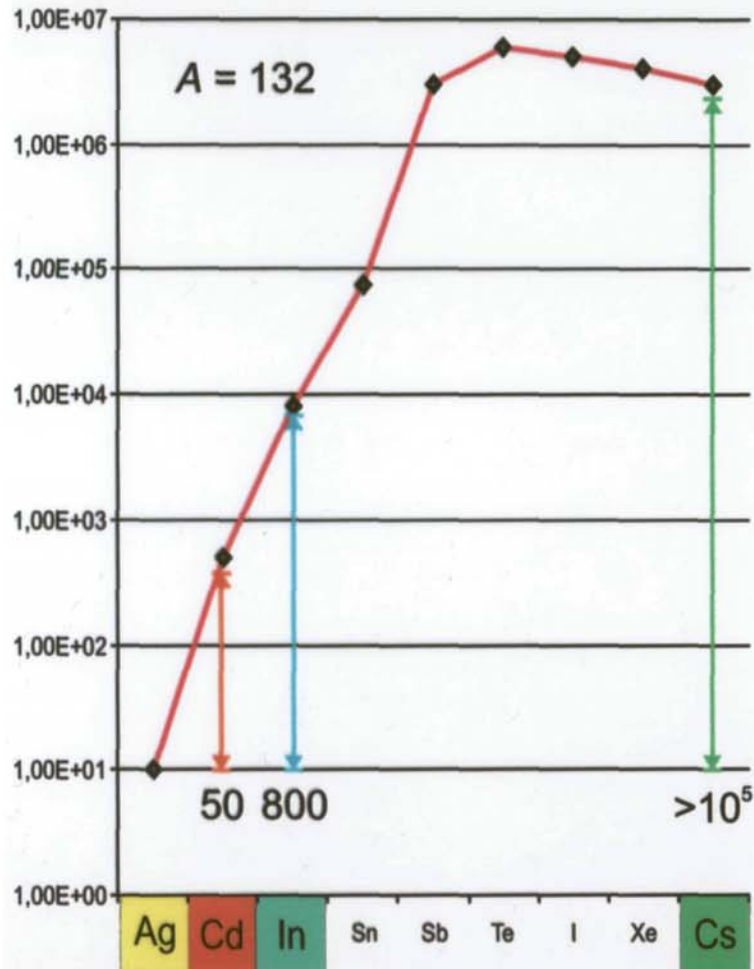
Fe-region	$N = 40, N = 50, Z = 28$ shell closures; r-process seed , α -rich freeze-out (?)
$A = 115$	deformation, shape transition $N > 66$; r-abundance trough
Sn-region	$N = 82, Z = 50$ shell closures; s.p.-structure around ^{132}Sn ; r-process waiting-point isotopes ; build-up, shape, matterflow out of $N_{r,e}$ -peak.

Experimental Setup



Relative production rates

Silberberg, Tsao



Selectivity

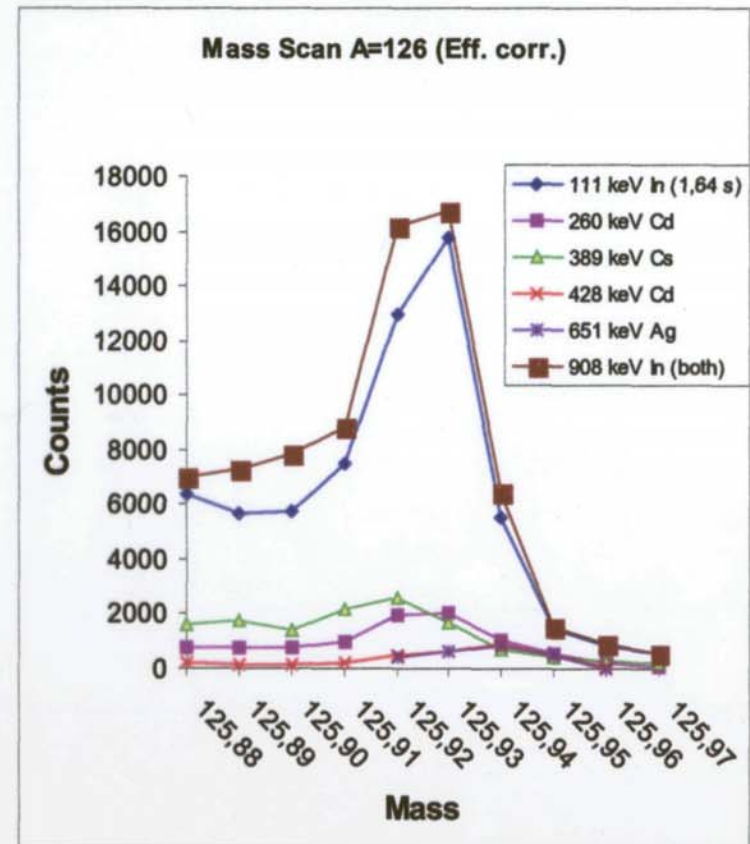
fast target

n-converter

LASER ion-scourer

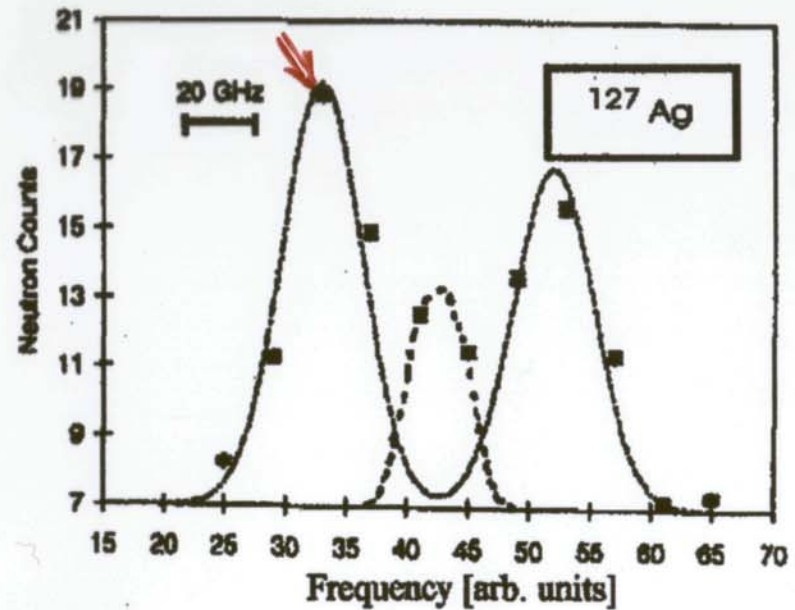
isobar separation

multi coincidence setup



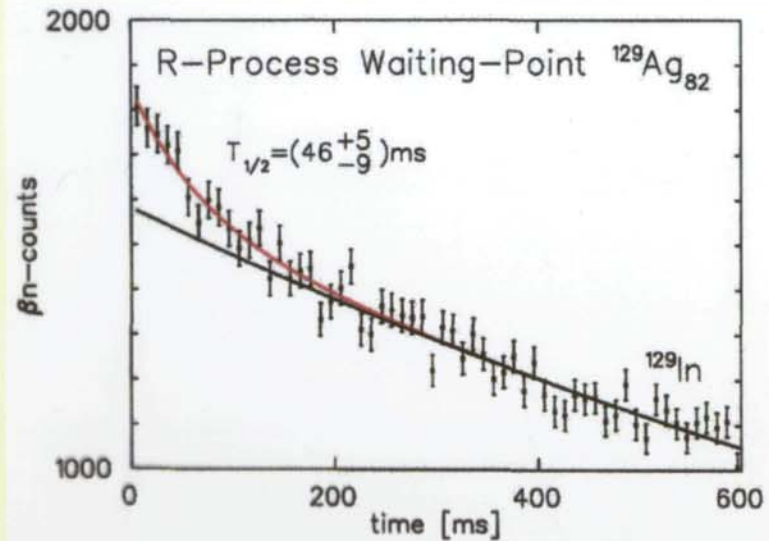
Additional selectivity from hyperfine splitting

- Solid line:
 - HF-splitting of the $\pi g_{9/2}$ configuration
- Dashed line:
 - $\pi p_{1/2}$ component

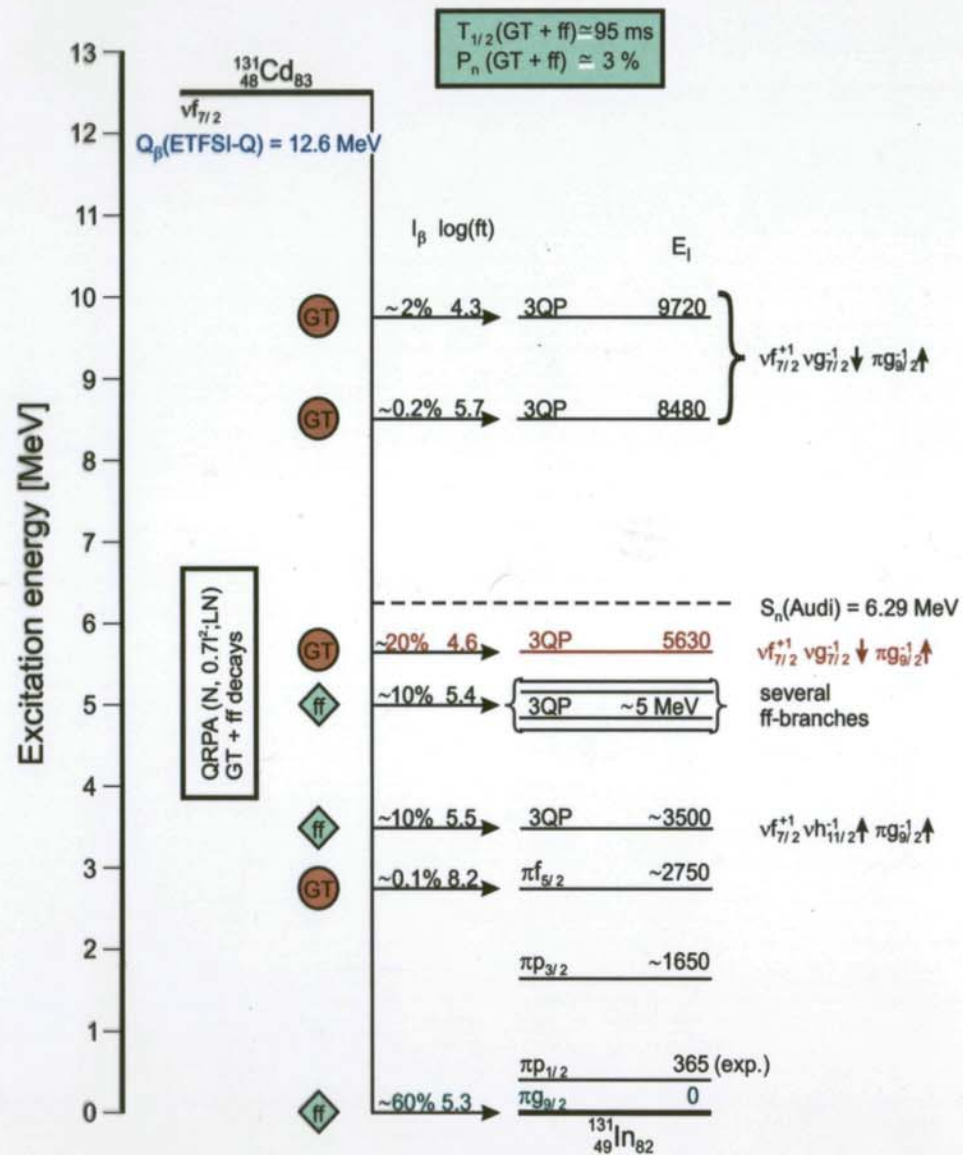
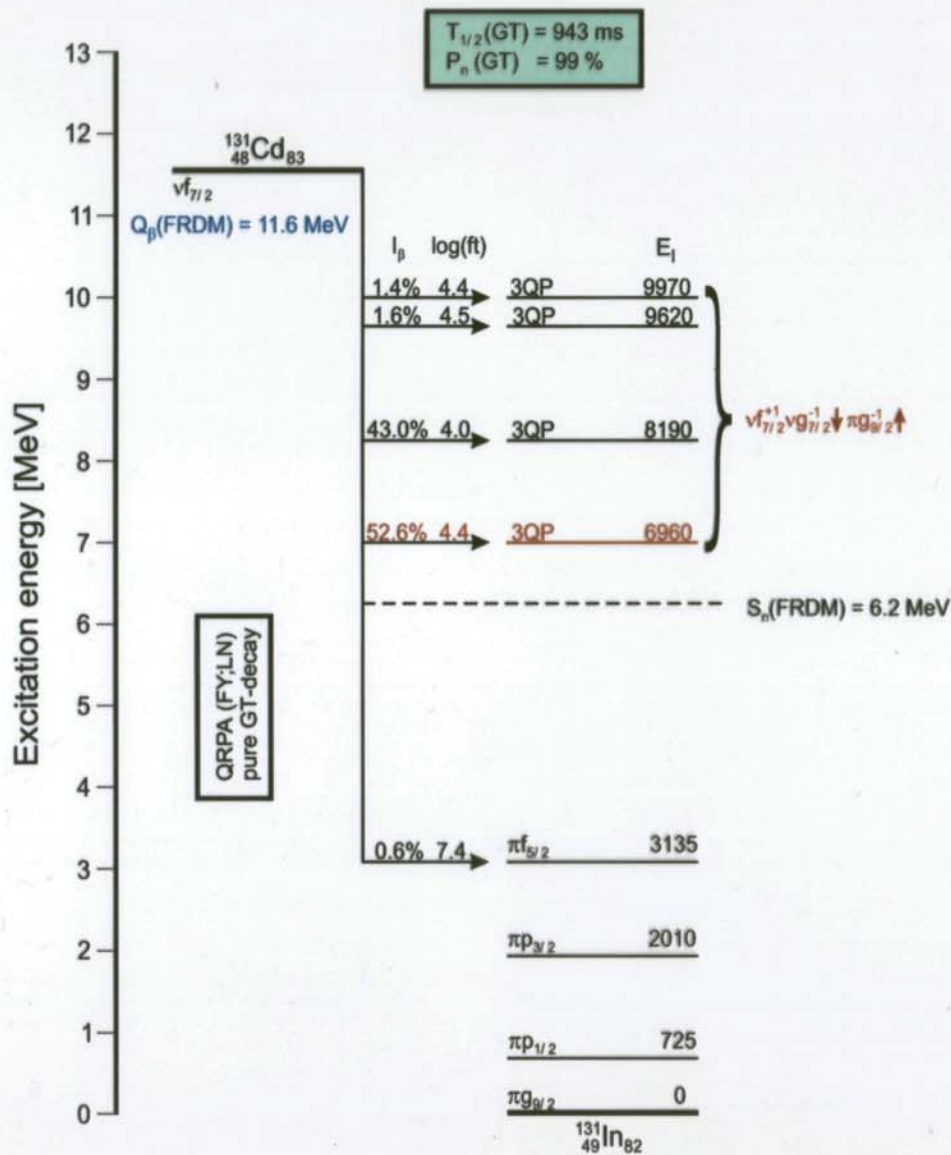


Laser ion source

- Laser set to off-center frequency
 $g_{9/2}$ ground-state decay
- Laser on central frequency
Indication of isomeric decay

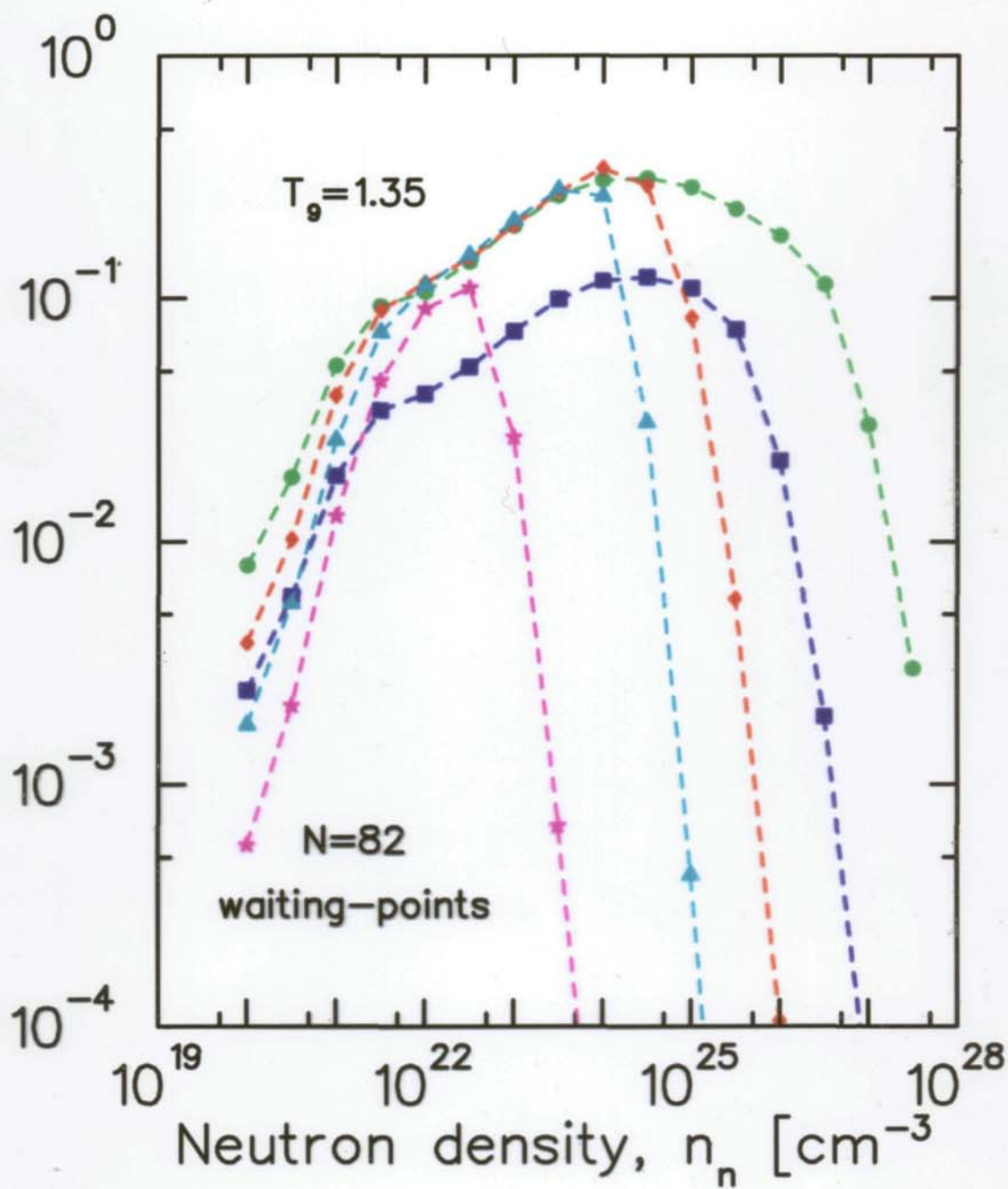


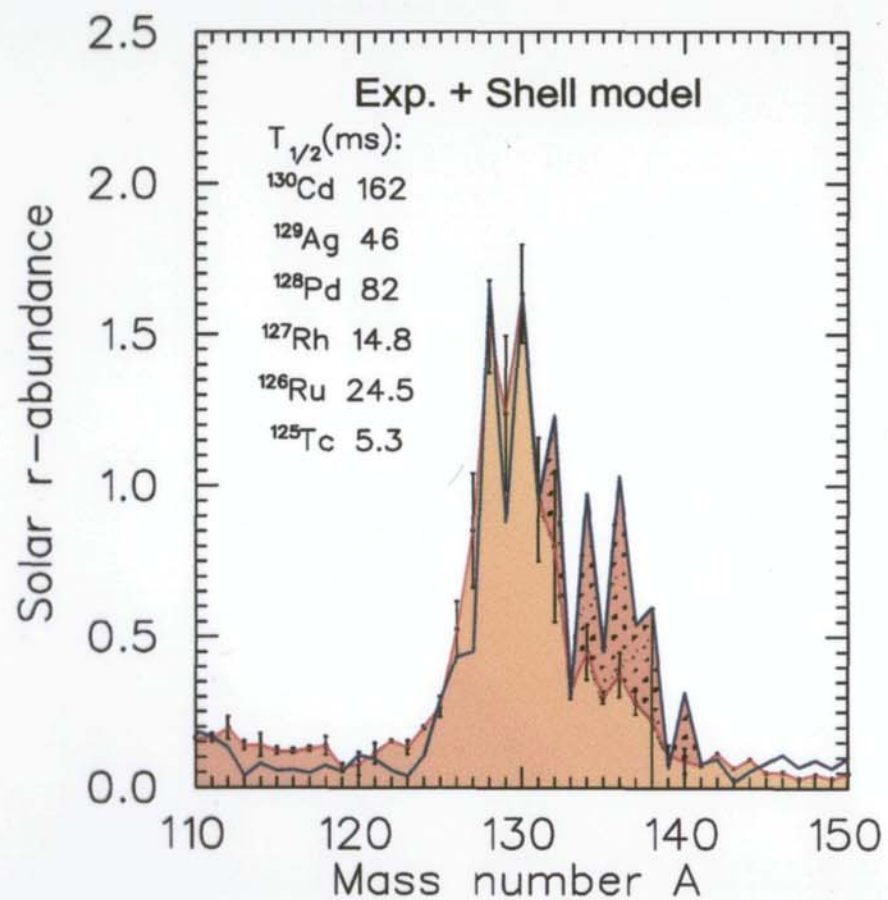
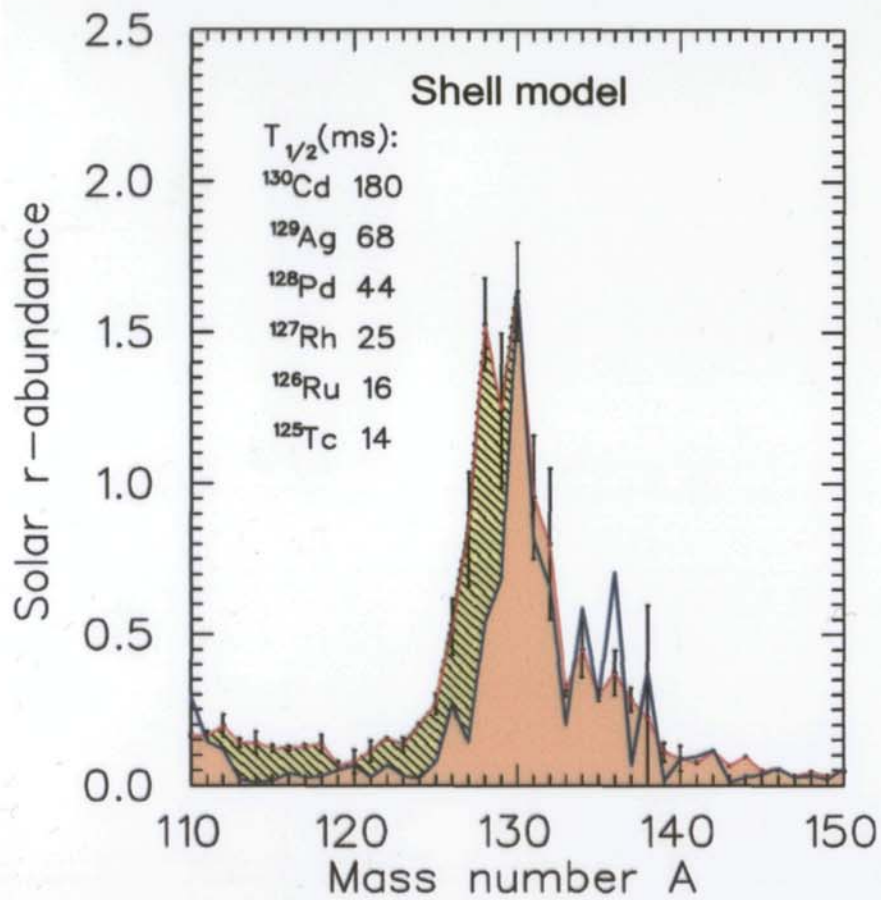
$$T_{1/2} = 68 \text{ ms}; P_n(\text{exp}) = 3.4 \%$$

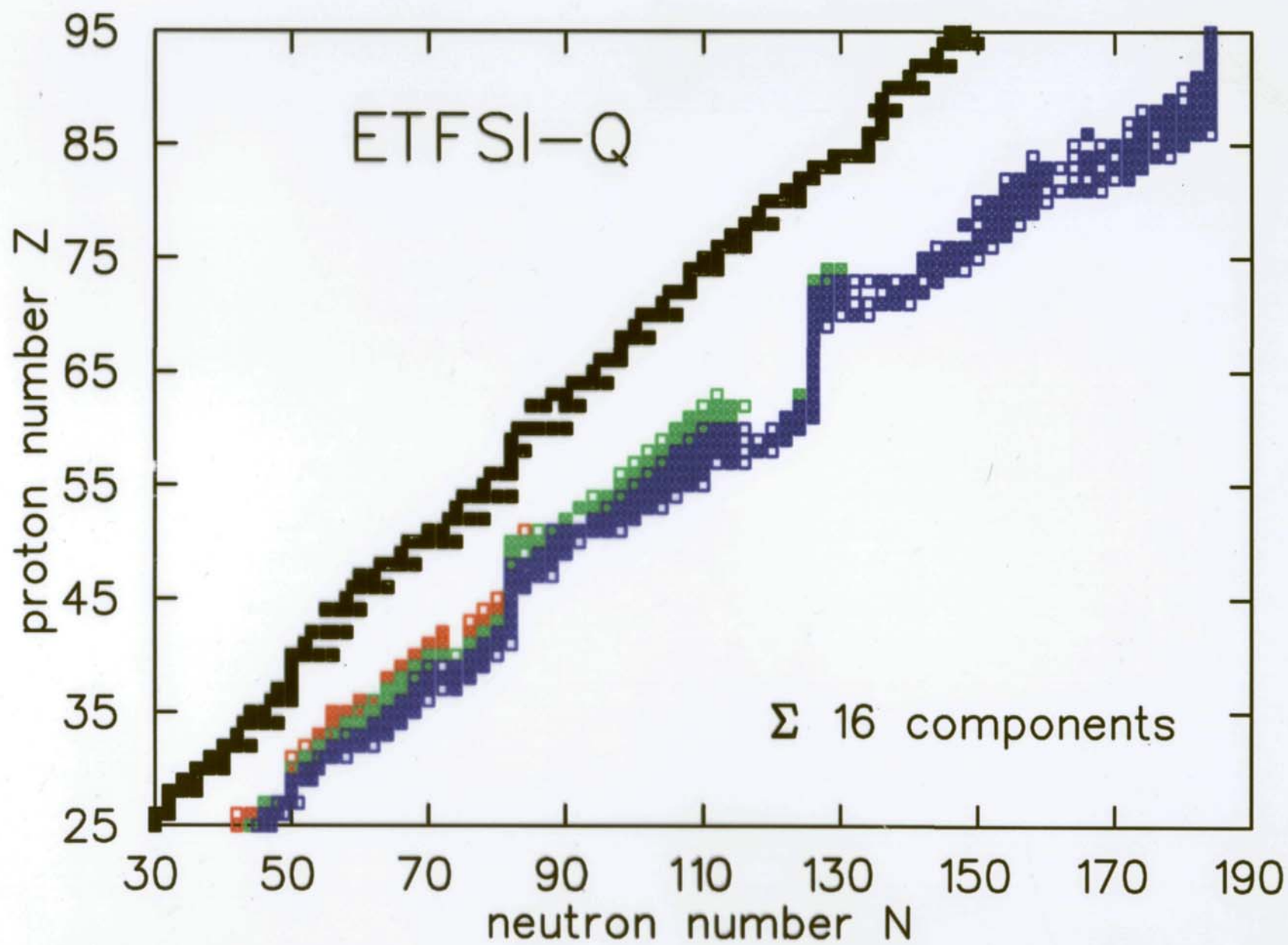


R-progenitor abundance, $N_{r, \text{prog}} [Si=10^0]$

- * ^{132}Sn
- \blacktriangle ^{131}In
- \blacklozenge ^{130}Cd
- \blacksquare ^{129}Ag
- \bullet ^{128}Pd







With this basis,

“application” of our r-abundance **calculations**
to recent **observations**

from Hubble Space Telescope (HST)
and high-resolution ground-based spectrographs
(e.g. KECK)

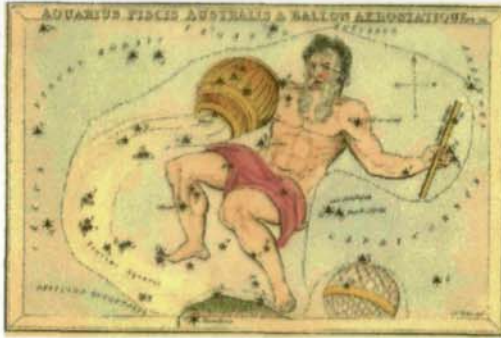
- **Elemental** abundances of UMP halo stars

Th,U cosmochronometers
age of the Universe

- **Isotopic** abundances in halo stars

stellar evolution of early Milky Way
r/s-process abundance mixtures
first stars → solar system

Determining the age of the Universe has long been considered the
“holy grail of cosmology”



BPS CS22892-052 in AQUARIUS
 RA 22:17:01.5 DE -16:39:26
 V=13.2, [Fe/H]=-3.1, dist.=4.7 kpc



HD115444 in CANES VENATICI
 RA 13:16:42.46 DE +36:22:53
 V=8.98, [Fe/H]=-3.0, dist.=286 pc



BPS CS31082-001 in CETUS
 RA 01:29:31.2 DE -16:00:48
 V=11.7, [Fe/H]=-2.9, dist.=4 kpc

HD122563 in BOÖTES

RA 14:02:31.8 DE +09:41:10

V=6.18, [Fe/H]=-2.7, dist.=266 pc

HD126238 in BOÖTES

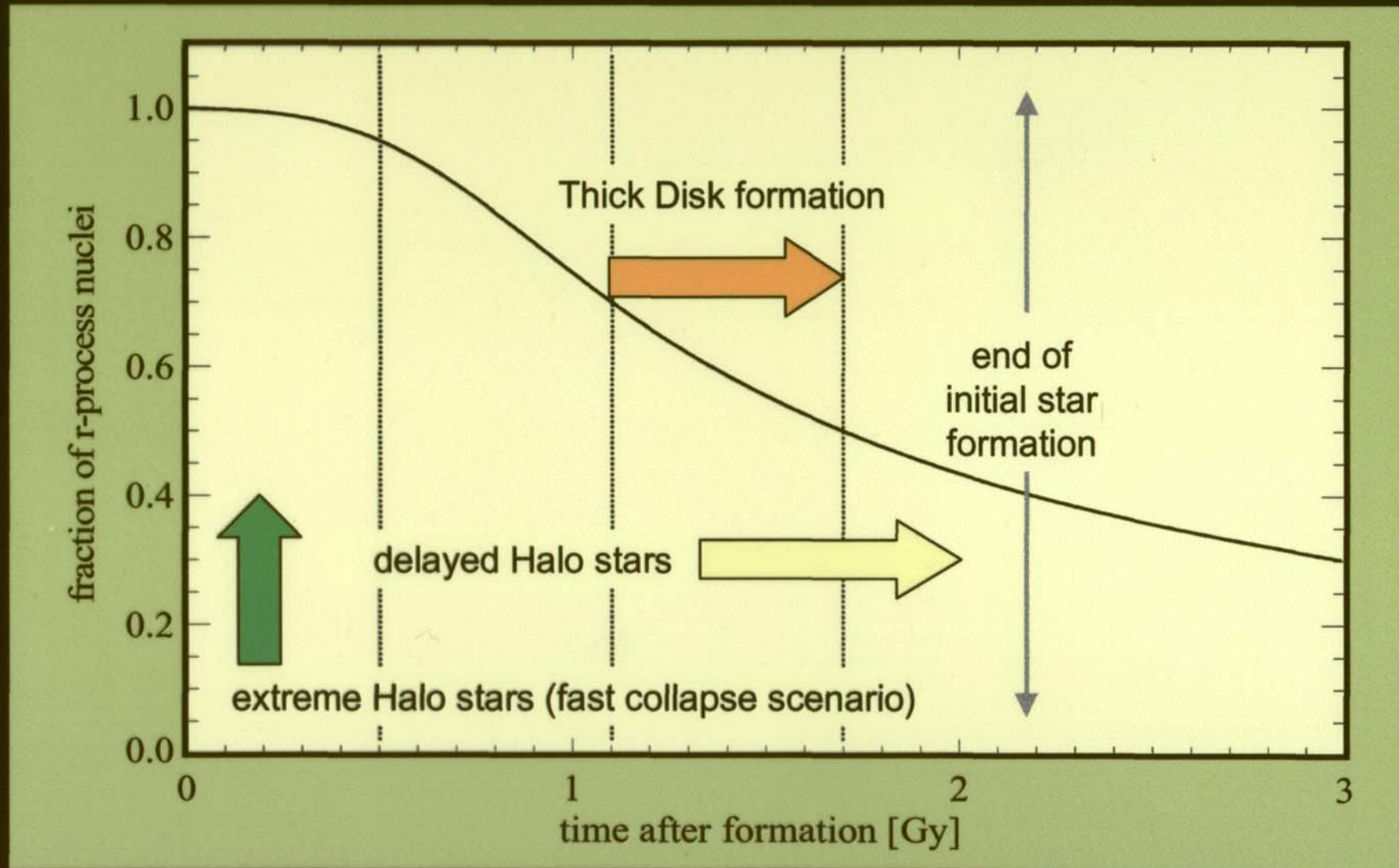
RA 14:25:30.0 DE +43:38:37

V=7.66, [Fe/H]=-1.7, dist.=263 pc

We compare r-process model predictions with recent astronomical observations from the solar system, ultra-metal-poor (UMP) halo stars and meteoritic r-process signatures, i.e. containing elemental as well as isotopic abundances. We deduce (1) astrophysical conditions (n_n -ranges for weak and main r-process components) under which such r-patterns can be obtained, and (2) criteria to determine Th/U chronometric ages.

These historic illustrations of the constellations are from Catherine Tennants *“The Box of Stars: A Practical Guide to the Night Sky and to Its Myths and Legends / Book, Cards and Maps.”* They are reproductions from *Urania’s Mirror*, published 1825 in London.

The early years of the Milky Way

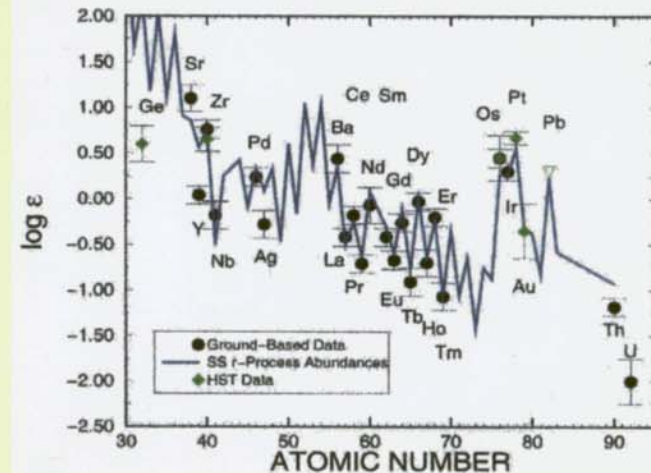


from Travaglio et al. (1999)

Ultra-metal-poor Halo stars

Th-U cosmochronometer

- Th-U chronometer ideal for dating of solar system.
- Lower limit for age of the Universe requires models of Galactic chemical evolution.
- High-resolution optical spectroscopy of ultra-metal-poor, very old Halo red giants stars opens new perspectives:
 - One (or few) nucleosynthesis events seeded ISM.
 - Scaled solar system r-process abundances for $56 \leq Z \leq 79$.
 - Radioactive dating requires „production ratios“.
 - Th/U ratio (hopefully) less effected by extrapolations of nuclear structure



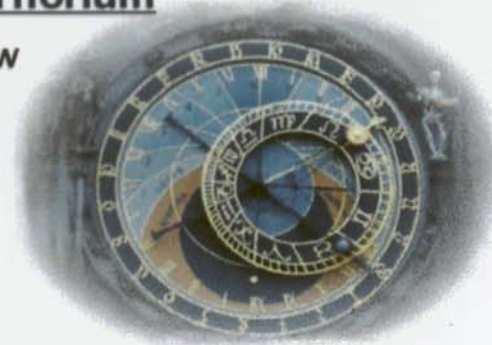
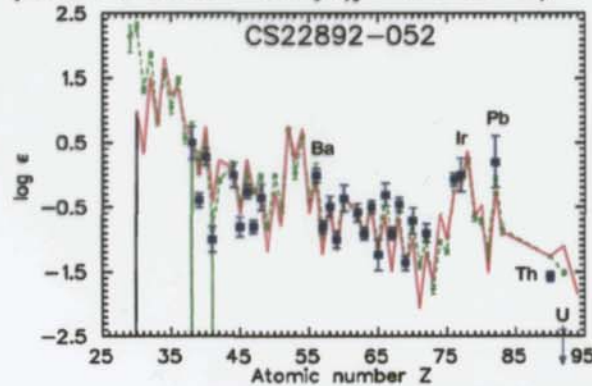
Abundances in BD+17°3248

Cosmochronology with Thorium

Several UMP halo stars consistently show solar elemental abundance pattern, among them

CS 22892-052

with 17 elements between Ba and Ir, plus Pb and ^{232}Th ($T_{1/2} = 14 \cdot 10^9 \text{ a}$)



📁 age from average of Th/Ba-Ir

$14.6 \pm 3.0 \text{ Gyr}$

🕒 age of the Universe

Tuning the clock with Uranium

Because of shorter half-life ($T_{1/2} = 4.5 \cdot 10^9 \text{ a}$), ^{238}U may yield more precise age.

Recently, first observation of U in CS 31082-001

(Cayrel et al., 2001)

📁 age from U/Th

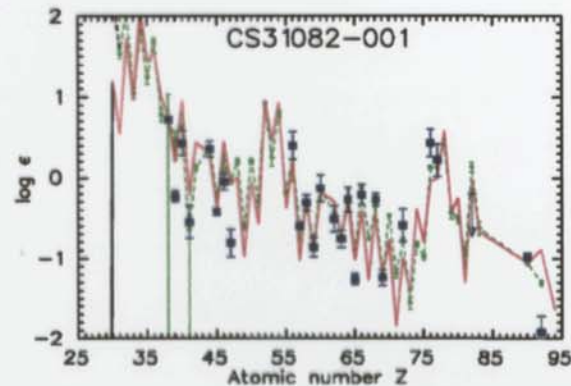
$15.0 \pm 3.0 \text{ Gyr}$

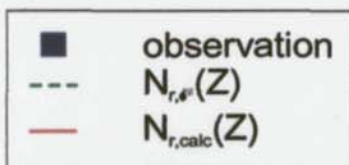
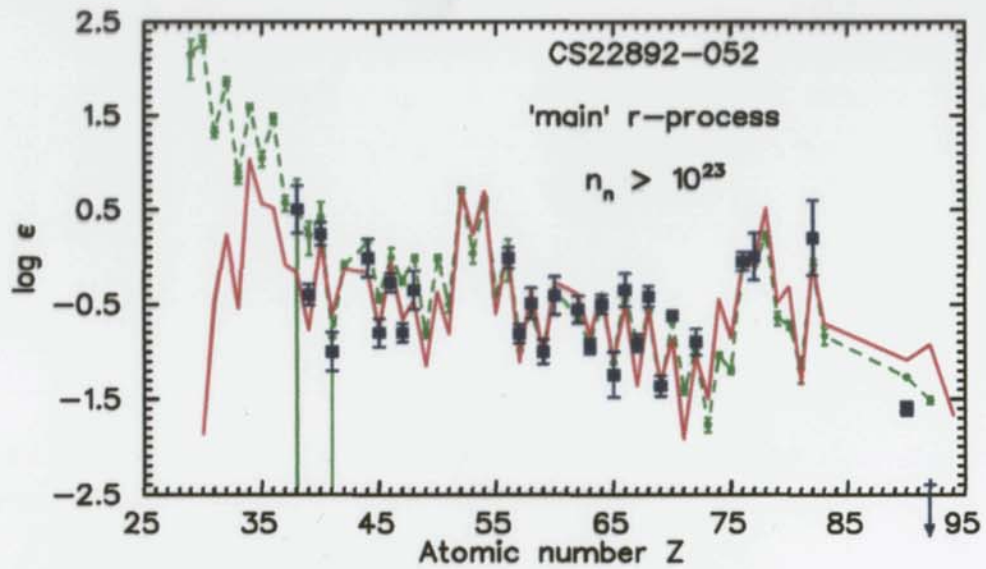
(Schatz et al., 2002)

In the meantime, second observation of U in BD +17°3248 📁 age from U/Th and U,Th/3rd peak

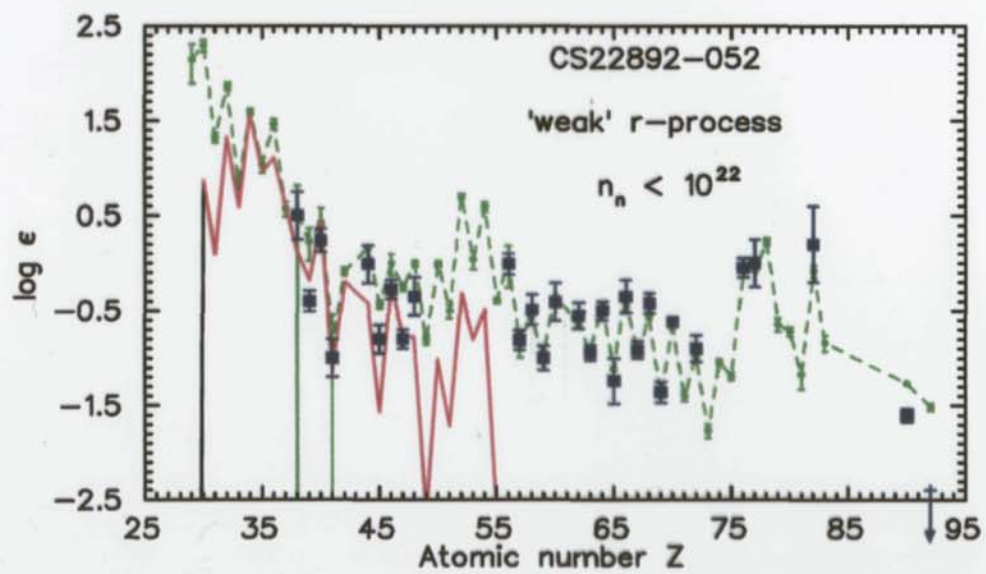
$13.8 \pm 4.0 \text{ Gyr}$

(Cowan et al., 2002)



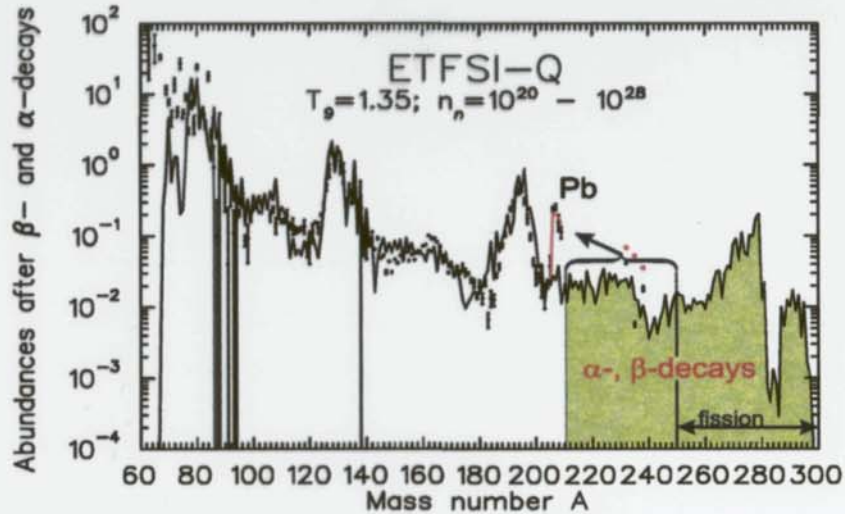


difference ($N_{r,obs}(Z) - N_{r,calc}(Z)$)
 = "weak" r-process



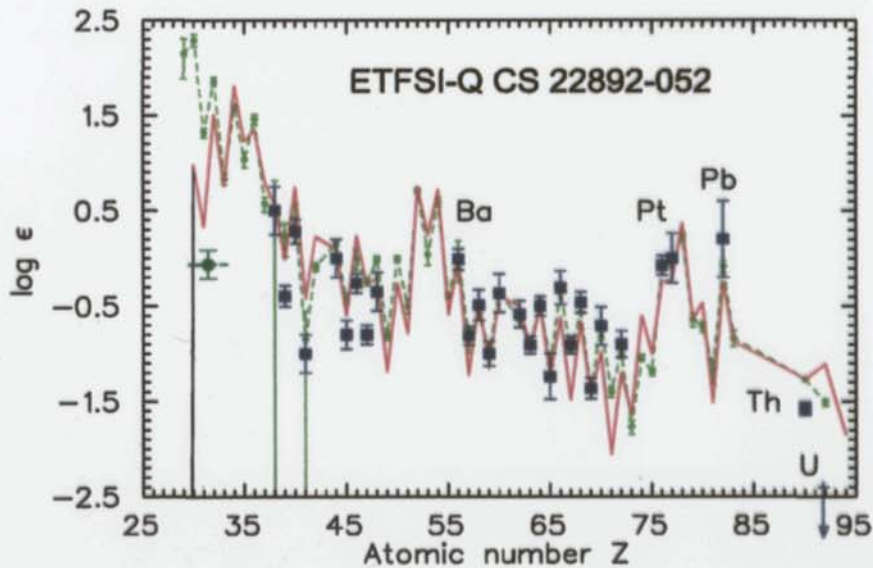
What do we calculate?

reproduce **isotopic** $N_{r,\odot}$ distribution
 using waiting-point approach
 (sq-fits; $A \geq 80$, $A \geq 120$)



Pb abundances as
 reliability criterion
 for Th, U region!

Convert to elemental $N_{r,\odot}$ curve(—), and scale to halo abundances (■)



↪ comparison to
 $N_{r,\odot}(Z)$

⇒ excellent
 agreement above
 Ba

⇒ Th, U cosmo-
 chronometry

s/r Isotopic Mixtures in UMP Halo Stars

Two recent cases:

① Sneden et al. (2002)

In 3 UMP stars, abundance ratio

$$^{153}\text{Eu} / ^{151}\text{Eu} \approx 1.0$$

to be compared to

$$^{153}\text{Eu}(s) / ^{151}\text{Eu}(s) = 0.85 \pm 0.09$$

$$^{153}\text{Eu}(r) / ^{151}\text{Eu}(r) = 1.11 \pm 0.02$$

possible s-process contamination difficult to identify

$$\rightarrow \text{Eu}(s) / \text{Eu}(r) \approx 6 / 94$$

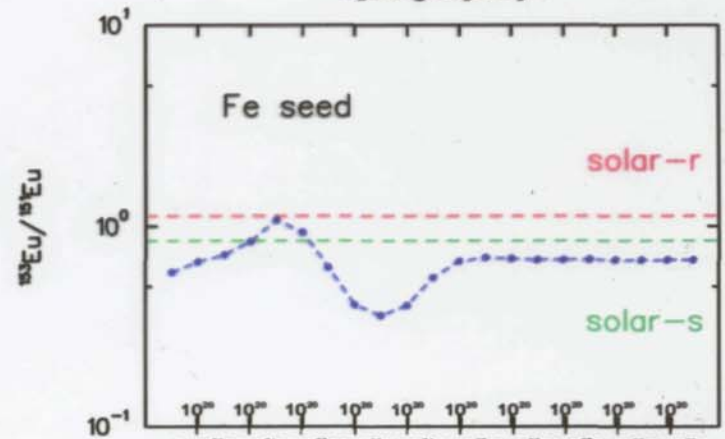
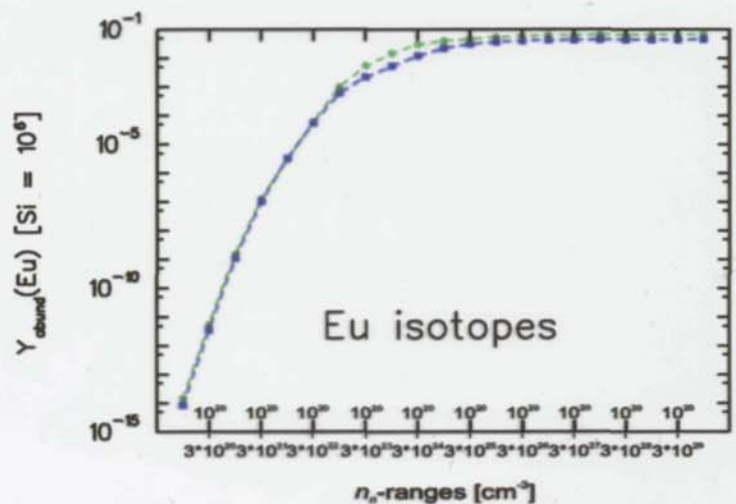
What do we calculate?

- Eu(r) as function of n_n -ranges

\rightarrow "main" r-process conditions

- calculated integral r-ratio

$$^{153}\text{Eu} / ^{151}\text{Eu} \approx 0.86$$



P. Magain (1995):

“the r/s-process controversy”

much stronger r/s constraints from isotopic abundances as a function of metallicity;
use isotopic hyperfine splitting, affecting line widths to determine odd-to-even isotopic ratios.

Barium is particularly well suited

Ba II spectral line at 4554 Å

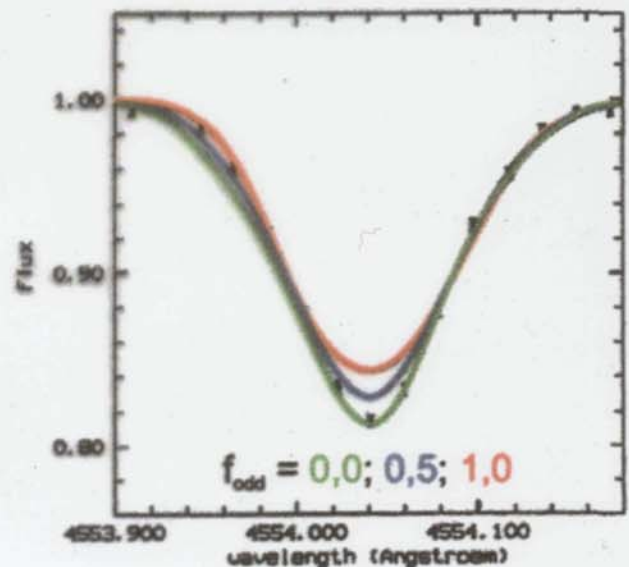
s-process dominates even isotopes ↪ narrow line

r-process dominates odd isotopes ↪ broad line

⇒ width of the line is a measure of the oe isotopic ratio, and thus of the r-process contribution.

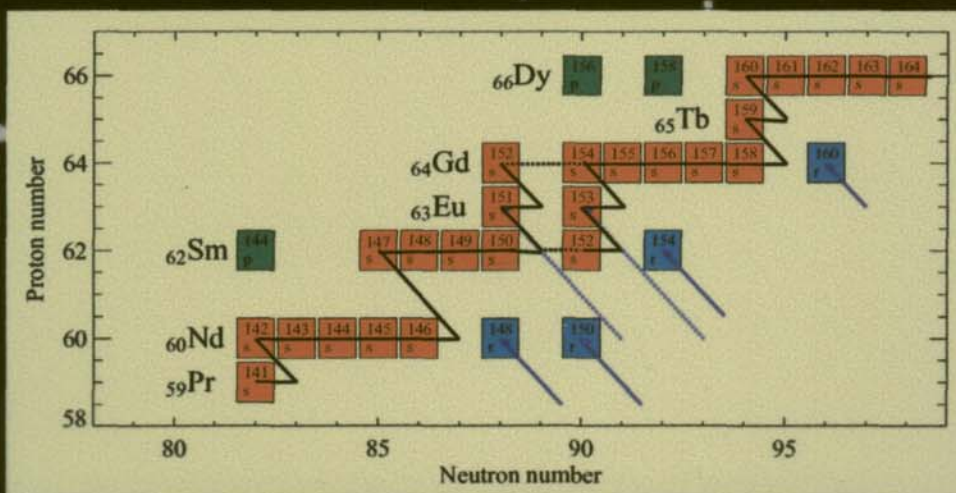
Definition:

$$f_{\text{odd}} = \frac{N(135\text{Ba}) + N(137\text{Ba})}{N(\text{Ba})}$$



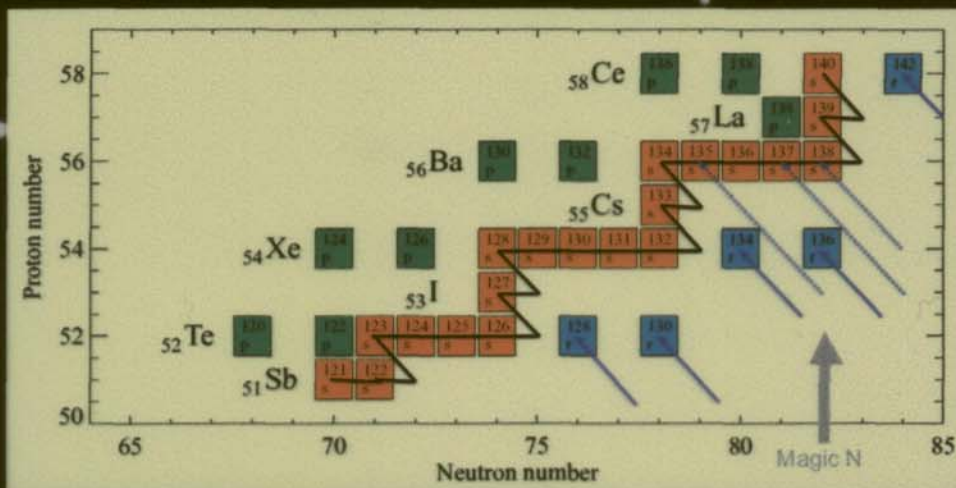
$$f_{\text{odd}}^{\odot} = 0.18 \pm 0.02 \quad f_{\text{odd}}^{s,\odot} = 0.11 \pm 0.02 \quad f_{\text{odd}}^{r,\odot} = 0.54 \pm 0.13$$

Europium isotopes and their nucleosynthesis



Europium isotopes are processed in a broken s-process chain. Both isotopes can be produced by the r-process, but also may have some s-process contributions.

Barium isotopes and their nucleosynthesis



Map of nuclides with valley of β -stability (s-process path). Also displays isotopes that can be produced in both s- and r-process (dotted arrows)

Analyses of 4554 Å line of HD 140283

P. Magain (1995)

$$f_{\text{odd}} = 0.08 \pm 0.06$$

"... in agreement with a pure **s-process** production ..."

D. L. Lambert (2002)

$$f_{\text{odd}} = 0.30 \pm 0.21$$

"... consistent with the solar **r-process** contributions to barium ..."

in addition,
from measured [Ba/Fe] and [Eu/Fe] ratios

$$\curvearrowright \text{ [Ba/Eu] } = -1.05$$

"... HD 140283 has the [Ba/Eu] ratio expected of the **r-process**;
... suggestion about **s-process** contamination ...(?)"

For **solar-like** r-process yields of Ba and Eu

$$\curvearrowright \text{ [Ba/Eu] } = -0.73 \pm 0.04$$

Definition:
$$[\text{Ba/Eu}] = \log \left[\frac{\text{Ba (r)}}{\text{Ba (}\odot\text{)}} / \frac{\text{Eu (r)}}{\text{Eu (}\odot\text{)}} \right]$$

What do we calculate?

① integral $f_{\text{odd}}^r(\text{Ba})$

average from 20 calculations ($10^{20} < n_n < 10^{30}$), using 11 different mass models / hybrid mass models and different global fit criteria to reproduce the overall isotopic $N_{r,\odot}$ pattern

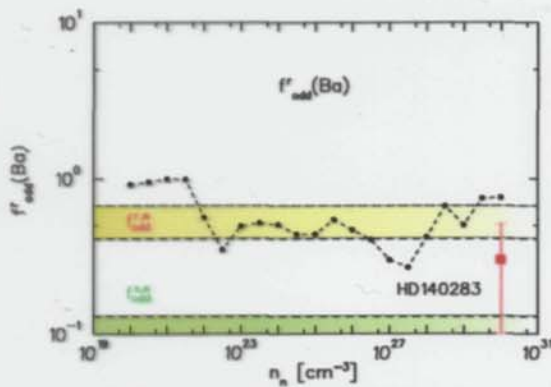
↪ quite robust result

$$f_{\text{odd}}^r(\text{Ba}) = 0.51 \pm 0.06$$

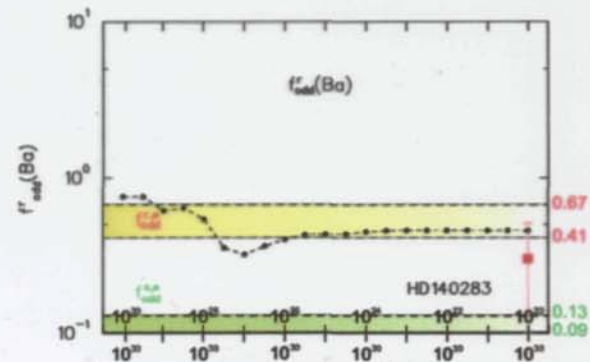
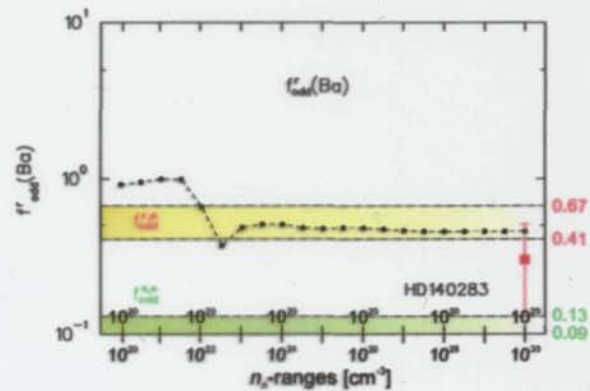
- good agreement with $f_{\text{odd}}^{r,\odot}(\text{Ba})$
- overlaps with upper limit of Lambert's $f_{\text{odd}}^r(\text{Ba})$ in HD 140283
- excludes $f_{\text{odd}}(\text{Ba}) < 0.4$

② $f_{\text{odd}}^r(\text{Ba})$ as function of neutron-density

(ETFSI-Q mass model)



individual n_n -components

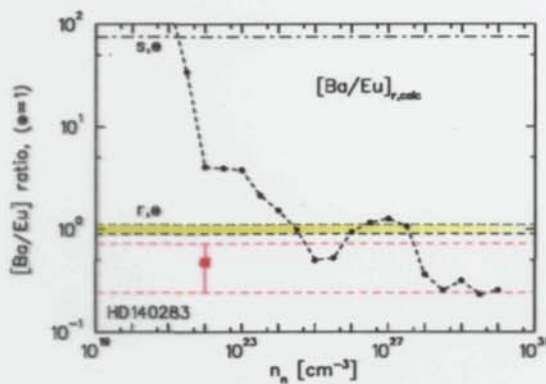


different n_n -ranges
... to simulate "weak"
and "main"
r-process conditions ...

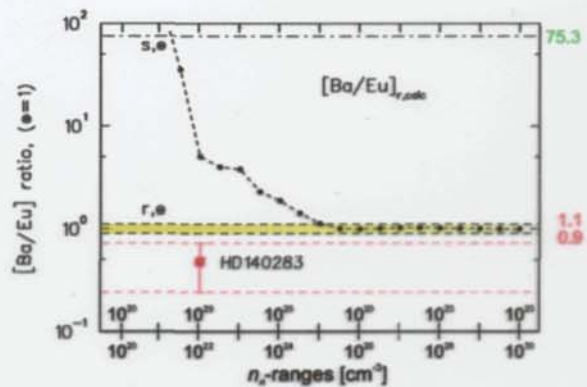
What do we calculate?

...ctd.

③ [Ba / Eu] as function of neutron-density
(ETFSI-Q mass model)

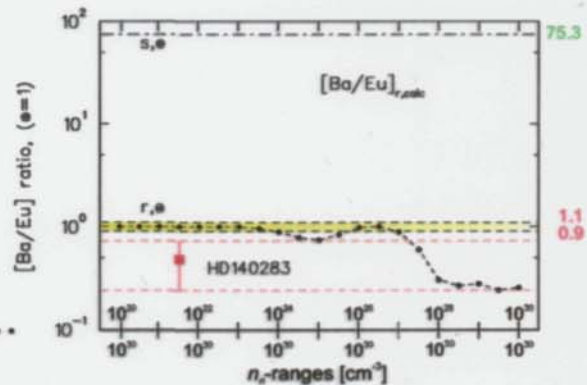


individual n_n -components



different n_n -ranges

... to simulate "weak"
and "main"
r-process conditions ...



Conclusions:

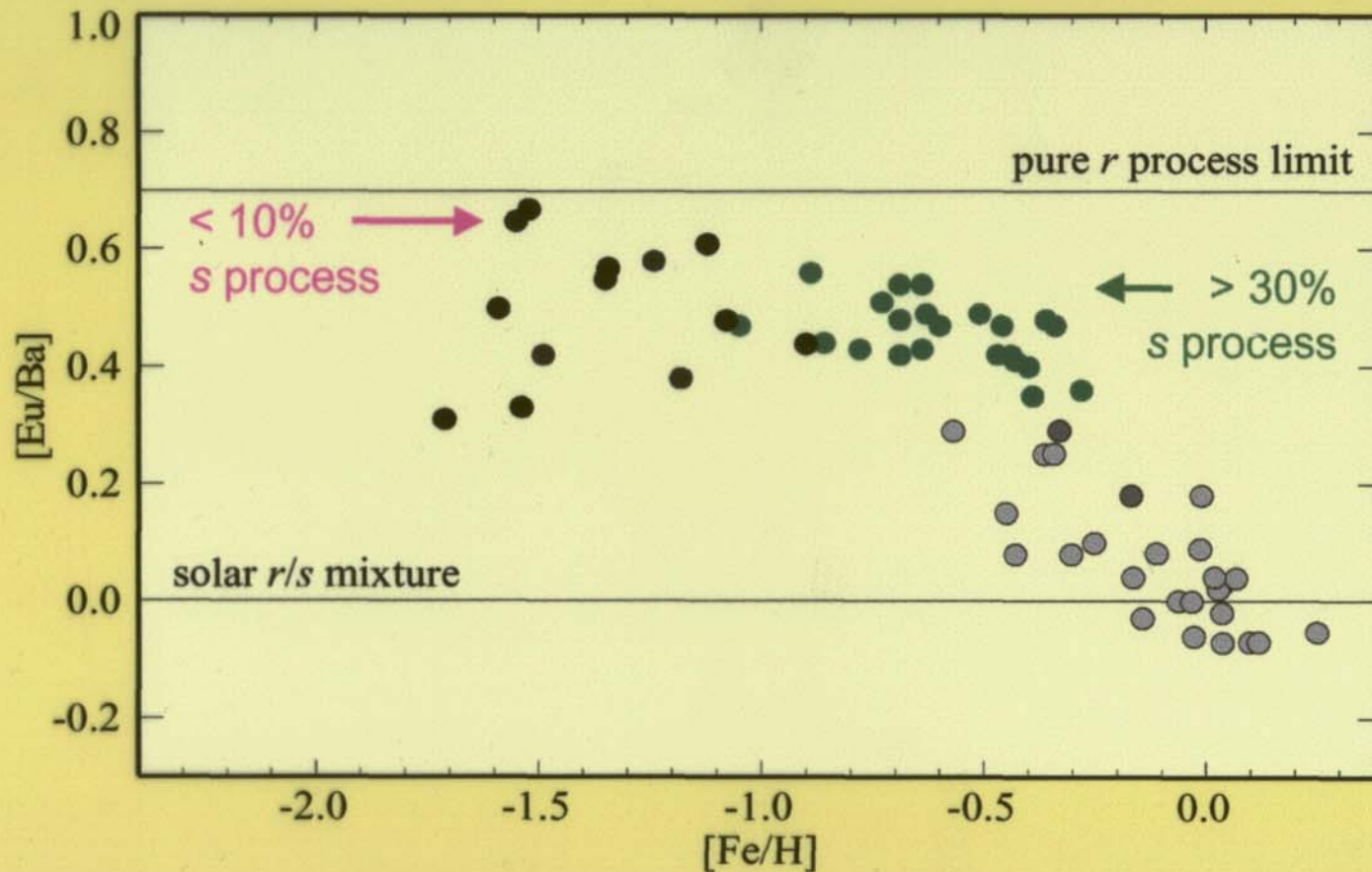
- measured $f_{\text{odd}}(\text{Ba}) = 0.30 \pm 0.21$

just in between f_{odd}^r and f_{odd}^s

- measured [Ba/Eu] = -1.05

favors high- n_n r-process
incompatible with s-process

- a "weak" r-process ($n_n < 10^{22}$) shows [Ba/Eu], similar to [Ba/Eu]_{s,calc}



Stellar evolution predicts the **first s nuclei 0.5 Gyr** after the proto-Galactic collapse, with another 0.6 Gyr to reach $s/r = 30 : 70$, and another 0.5 Gyr to arrive at $50 : 50$

Conclusions

Direct comparison between astronomical and nuclear structure **observations** and astro-model predictions

- information about stellar parameters
 - temperatures,
 - particle (e.g. p, α , n) and matter densities,
 - time scales,
 - hydrodynamical conditions
- possible information on nuclear physics far from stability
 - position of particle drip-lines
 - regions of shape transition
 - monopole shifts
 - shell quenching

It is clear that also in the future astrophysics will have to rely on nuclear physics input; mainly from nuclear theories, still not sufficiently well understood.

Therefore, continued **request** for

radioactive-beam
nuclear mass
 β -decay

experiments

Present ISOL-RIB facilities
(ISOLDE, SPIRAL, ...)

